VELOCITY-VORTICITY-PRESSURE FORMULATION FOR THE OSEEN PROBLEM WITH VARIABLE VISCOSITY*

V. ANAYA†, R. CARABALLO‡, B. GÓMEZ-VARGAS§, D. MORA¶, AND R. RUIZ-BAIER‖

Abstract. We propose and analyse an augmented mixed finite element method for the Oseen equations written in terms of velocity, vorticity, and pressure with non-constant viscosity and homogeneous Dirichlet boundary condition for the velocity. The weak formulation includes least-squares terms arising from the constitutive equation and from the incompressibility condition, and we show that it satisfies the hypotheses of the Babuška-Brezzi theory. Repeating the arguments of the continuous analysis, the stability and solvability of the discrete problem are established. The method is suited for any Stokes inf-sup stable finite element pair for velocity and pressure, while for vorticity any generic discrete space (of arbitrary order) can be used. A priori and a posteriori error estimates are derived using two specific families of discrete subspaces. Finally, we provide a set of numerical tests illustrating the behaviour of the scheme, verifying the theoretical convergence rates, and showing the performance of the adaptive algorithm guided by residual a posteriori error estimation.

Key words. Oseen equations, velocity-vorticity-pressure formulation, mixed finite element methods, variable viscosity, a priori and a posteriori error analysis, adaptive mesh refinement.

AMS subject classifications. 65N30, 65N12, 76D07, 65N15.

1. Introduction. Using vorticity as additional field in the formulation of incompressible flow equations can be advantageous in a number of applicative problems [47]. Starting from the seminal works [25, 26] that focused on Stokes equations and where vorticity was sought in H($\mathbf{curl}, \Omega$), several different problems including Brinkman, Navier-Stokes, and related flow problems written in terms of vorticity have been studied from the viewpoint of numerical analysis of finite volume and mixed finite element methods exhibiting diverse properties and specific features. Some of these contributions include [3, 2, 4, 7, 23, 12, 45, 46].

The starting point is the Oseen equations in the case of variable viscosity, and written in terms of velocity $\boldsymbol{u}$ and pressure p, as follows (see [35]):

$$\sigma\boldsymbol{u} - 2\mathbf{div}(\nu\boldsymbol{\varepsilon}(\boldsymbol{u})) + (\boldsymbol{\beta}\cdot\nabla)\boldsymbol{u} + \nabla p = \boldsymbol{f} \qquad \text{in } \Omega, \qquad (1.1\text{a})$$

$$\operatorname{div}\boldsymbol{u} = 0 \qquad \text{in } \Omega, \qquad (1.1\text{b})$$

$$\boldsymbol{u} = \boldsymbol{0} \qquad \text{on } \Gamma, \qquad (1.1\text{c})$$

$$(p, 1)_{0,\Omega} = 0, \qquad (1.1\text{d})$$

where $\sigma > 0$ is inversely proportional to the time-step, $\boldsymbol{f} \in \mathrm{L}^2(\Omega)^d$ is a force density, $\boldsymbol{\beta} \in \mathrm{H}^1(\Omega)^d$ is the convecting velocity field (not necessarily divergence-free), and $\nu \in W^{1,\infty}(\Omega)$ is the kinematic viscosity of the fluid, satisfying

$$0 < \nu_0 \leq \nu \leq \nu_1. \qquad (1.2)$$

Such a set of equations will appear, for instance, in the linearisation of non-Newtonian flow problems, as well as in applications where viscosity may depend on temperature, concentration or volume

†GIMNAP, Departamento de Matemática, Universidad del Bío-Bío, Concepción, Chile and CI²MA, Universidad de Concepción, Concepción, Chile (vanaya@ubiobio.cl).

‡GIMNAP, Departamento de Matemática, Universidad del Bío-Bío, Concepción, Chile (ruben.caraballo1801@alumnos.ubiobio.cl).

§Sección de Matemática, Sede de Occidente, Universidad de Costa Rica, San Ramón de Alajuela, Costa Rica (bryan.gomezvargas@ucr.ac.cr).

¶GIMNAP, Departamento de Matemática, Universidad del Bío-Bío, Concepción, Chile and CI²MA, Universidad de Concepción, Concepción, Chile (dmora@ubiobio.cl).

‖School of Mathematical Sciences, Monash University, 9 Rainforest Walk, Melbourne VIC 3800, Australia; and Universidad Adventista de Chile, Casilla 7-D, Chillán, Chile (ricardo.ruizbaier@monash.edu).

fractions, or other fields where the fluid flow patterns depend on marked spatial distributions of viscosity [37, 41, 42, 44]. The specific literature related to the analysis of numerical schemes for the Oseen equations in terms of vorticity includes the non-conforming exponentially accurate least-squares spectral method proposed in [40], least-squares methods proposed in [48] for Oseen and Navier-Stokes equations with velocity boundary conditions, the family of vorticity-based first-order Oseen-type systems studied in [21], the enhanced accuracy formulation in terms of velocity-vorticity-helicity investigated in [11], and the recent mixed (exactly divergence-free) and DG discretisations for Oseen's problem in velocity-vorticity-pressure form given in [5]. However, in most of these references, the derivation of the variational formulations depends on the viscosity being constant. This is attributed to the fact that the usual vorticity-based weak formulation results from exploiting the following identity

$$\mathbf{curl}(\mathbf{curl}\,\boldsymbol{v}) = -\Delta\boldsymbol{v} + \nabla(\operatorname{div}\boldsymbol{v}), \tag{1.3}$$

applied to the viscous term. However for a more general friction term of the form $-\mathbf{div}(\nu\boldsymbol{\varepsilon}(\boldsymbol{u}))$, where $\boldsymbol{\varepsilon}(\boldsymbol{u})$ is the strain rate tensor, the decomposition gives other additional terms that do not permit the direct recasting of the coupled system as done in the cited references above.

Extensions to cover the case of variable viscosity do exist in the literature. For instance, [27] addresses the well-posedness of the vorticity–velocity formulation of the Stokes problem with varying density and viscosity, and the equivalence of the vorticity–velocity and velocity–pressure formulations in appropriate functional spaces is proved. More recently, in [6] we have taken a different approach and employed an augmented vorticity-velocity-pressure formulation for Brinkman equations with variable viscosity. Here we extend that analysis to the generalised Oseen equations with variable viscosity, and address in particular how to deal with the additional challenges posed by the presence of the convective term that did not appear in the Brinkman momentum equation.

We will employ the so-called augmented formulations (also known as Galerkin least-squares methods), which can be regarded as a stabilisation technique where some terms are added to the variational formulation. Augmented finite elements have been considered in several works with applications in fluid mechanics (see, e.g., [8, 9, 13, 20, 17, 18, 34, 43] and the references therein). These methods enjoy appealing advantages as those described in length in, e.g., [14, 16], and reformulations of the set of equations following this approach are also of great importance in the design of block preconditioners (see [10, 31] for an application in Oseen and Navier-Stokes equations in primal form, [30] for stress-velocity-pressure formulations for non-Newtonian flows, or [19, 29] for stress-displacement-pressure mixed formulations for hyperelasticity). In the particular context of our mixed formulation for Oseen equations, the augmentation assists us in deriving the Babuška-Brezzi property of ellipticity on the kernel needed for the top-left diagonal block.

The formulation that we employ is non-symmetric, and the augmentation terms appear from least-squares contributions associated with the constitutive equation and the incompressibility constraint. The mixed variational formulation is shown to be well-posed under a condition on the viscosity bounds (a generalisation of the usual condition needed in Oseen equations, (cf. Theorem 2.4 and Remark 2.6). Then we establish the well-posedness of the discrete problem for generic inf-sup stable finite elements (for velocity and pressure) in combination with a generic space for vorticity approximation. We obtain error estimates for two stable families of finite elements. We also derive a reliable and efficient residual-based a posteriori error estimator for the mixed problem, which can be fully computed locally. In summary, the advantages of the proposed method are the possibility to obtain directly the vorticity field with optimal accuracy and without the need of postprocessing; moreover, different from many existing finite element methods with vorticity field as unknown, the present contribution supports variable viscosity and no-slip boundary condition in a natural way.

The contents of the paper have been structured as follows. Functional spaces and recurrent notation is collected in the remainder of this section. Section 2 presents the governing equations in terms of velocity, vorticity and pressure; we state an augmented formulation, and we perform the solvability analysis invoking the Babuška–Brezzi theory. The finite element discretisation is introduced in Section 3, where we also derive the stability analysis and optimal error estimates for two families of stable elements. In Section 4, we develop the a posteriori error analysis. Several numerical tests illustrating the convergence of the proposed method under different scenarios are

reported in Section 5.

Preliminaries. Let Ω be a bounded domain of $\mathbb{R}^d$, $d = 2, 3$, with Lipschitz boundary $\Gamma = \partial\Omega$. For any $s \geq 0$, the notation $\|\cdot\|_{s,\Omega}$ stands for the norm of the Hilbertian Sobolev spaces $H^s(\Omega)$ or $H^s(\Omega)^d$, with the usual convention $H^0(\Omega) := L^2(\Omega)$.

Moreover, c and C, with or without subscripts, tildes, or hats, will represent a generic constant independent of the mesh parameter h, assuming different values in different occurrences. In addition, for any vector field $\boldsymbol{v} = (v_i)_{i=1}^3$ and any scalar field q we recall the notation:

$$\operatorname{div}\boldsymbol{v} = \sum_{i=1}^3 \partial_i v_i, \ \ \mathbf{curl}\,\boldsymbol{v} = \begin{pmatrix} \partial_2 v_3 - \partial_3 v_2 \\ \partial_3 v_1 - \partial_1 v_3 \\ \partial_1 v_2 - \partial_2 v_1 \end{pmatrix}, \ \ \nabla q = \begin{pmatrix} \partial_1 q \\ \partial_2 q \\ \partial_3 q \end{pmatrix},$$

whereas for dimension $d = 2$, the curl of a vector $\boldsymbol{v}$ and a scalar q are scalar function $\partial_1 v_2 - \partial_2 v_1$ and the vector $\mathbf{curl}\, q = (\partial_2 q, \partial_1 q)^t$, respectively.

Recall that, according to [35, Theorem 2.11], for a generic domain $\Omega \subseteq \mathbb{R}^3$, the relevant integration by parts formula corresponds to

$$\int_\Omega \mathbf{curl}\,\boldsymbol{\omega} \cdot \boldsymbol{v} = \int_\Omega \boldsymbol{\omega} \cdot \mathbf{curl}\,\boldsymbol{v} + \langle \boldsymbol{\omega} \times \boldsymbol{n}, \boldsymbol{v} \rangle_\Gamma,$$

which in 2D reads as

$$\int_\Omega \mathbf{curl}\,\omega \cdot \boldsymbol{v} = \int_\Omega \omega\,\mathbf{curl}\,\boldsymbol{v} - \langle \boldsymbol{v} \cdot \boldsymbol{t}, \omega \rangle_\Gamma. \tag{1.4}$$

2. Vorticity-based formulation. With the aim of proposing a vorticity-based formulation for (1.1), we consider the following identities

$$-2\mathbf{div}(\nu\boldsymbol{\varepsilon}(\boldsymbol{u})) = -2\nu\mathbf{div}(\boldsymbol{\varepsilon}(\boldsymbol{u})) - 2\boldsymbol{\varepsilon}(\boldsymbol{u})\nabla\nu = -\nu\Delta\boldsymbol{u} - 2\boldsymbol{\varepsilon}(\boldsymbol{u})\nabla\nu$$
$$= \nu\,\mathbf{curl}(\mathbf{curl}\,\boldsymbol{u}) - \nu\nabla(\operatorname{div}\boldsymbol{u}) - 2\boldsymbol{\varepsilon}(\boldsymbol{u})\nabla\nu.$$

Therefore, problem (1.1) rewrites as

$$\sigma\boldsymbol{u} + \nu\,\mathbf{curl}\,\boldsymbol{\omega} - 2\boldsymbol{\varepsilon}(\boldsymbol{u})\nabla\nu + (\boldsymbol{\beta}\cdot\nabla)\boldsymbol{u} + \nabla p = \boldsymbol{f} \qquad \text{in } \Omega, \tag{2.5a}$$
$$\boldsymbol{\omega} - \mathbf{curl}\,\boldsymbol{u} = \boldsymbol{0} \qquad \text{in } \Omega, \tag{2.5b}$$
$$\operatorname{div}\boldsymbol{u} = 0 \qquad \text{in } \Omega, \tag{2.5c}$$
$$\boldsymbol{u} = \boldsymbol{0} \qquad \text{on } \Gamma, \tag{2.5d}$$
$$(p, 1)_{0,\Omega} = 0, \tag{2.5e}$$

where we have considered the definition of the vorticity and have applied the incompressibility condition. The equations state, respectively, the momentum conservation, the constitutive relation, the mass balance, the no-slip boundary condition, and the pressure closure condition.

2.1. Variational formulation for the Oseen equations with non-constant viscosity. In this section, we propose a mixed variational formulation of system (2.5a)-(2.5e). First, we endow the space $H_0^1(\Omega)^d$ with the following norm:

$$\|\boldsymbol{v}\|_{1,\Omega}^2 := \|\boldsymbol{v}\|_{0,\Omega}^2 + \|\mathbf{curl}\,\boldsymbol{v}\|_{0,\Omega}^2 + \|\operatorname{div}\boldsymbol{v}\|_{0,\Omega}^2,$$

and note that for $H_0^1(\Omega)^d$ the above norm is equivalent to the usual norm. In particular, we have that there exists a positive constant C_{pf} such that:

$$\|\boldsymbol{v}\|_{1,\Omega}^2 \leq C_{pf}(\|\mathbf{curl}\,\boldsymbol{v}\|_{0,\Omega}^2 + \|\operatorname{div}\boldsymbol{v}\|_{0,\Omega}^2) \qquad \forall \boldsymbol{v} \in H_0^1(\Omega)^d,$$

where the above inequality is a consequence of the identity

$$\|\nabla\boldsymbol{v}\|_{0,\Omega}^2 = \|\mathbf{curl}\,\boldsymbol{v}\|_{0,\Omega}^2 + \|\operatorname{div}\boldsymbol{v}\|_{0,\Omega}^2. \tag{2.6}$$

which follows from (1.3) and the Poincaré inequality. Moreover, in order to establish a weak formulation for (2.5), we will use the following identity:

$$\mathbf{curl}(\phi \boldsymbol{v}) = \nabla \phi \times \boldsymbol{v} + \phi\, \mathbf{curl}\, \boldsymbol{v}, \tag{2.7}$$

valid for any vector field $\boldsymbol{v}$ and any scalar field ϕ.

After testing each equation of (2.5a)-(2.5d) against adequate functions, using (2.7), and imposing the boundary conditions, we end up with the following system:

$$\int_\Omega (\sigma \boldsymbol{u} + (\boldsymbol{\beta} \cdot \nabla)\boldsymbol{u}) \cdot \boldsymbol{v} - 2 \int_\Omega \boldsymbol{\varepsilon}(\boldsymbol{u})\nabla\nu \cdot \boldsymbol{v} + \int_\Omega \nu\boldsymbol{\omega} \cdot \mathbf{curl}\, \boldsymbol{v} + \int_\Omega \boldsymbol{\omega} \cdot (\nabla\nu \times \boldsymbol{v}) - \int_\Omega p\, \mathrm{div}\, \boldsymbol{v} = \int_\Omega \boldsymbol{f} \cdot \boldsymbol{v},$$

$$\int_\Omega \nu\boldsymbol{\theta} \cdot \mathbf{curl}\, \boldsymbol{u} - \int_\Omega \nu\boldsymbol{\omega} \cdot \boldsymbol{\theta} = 0,$$

$$- \int_\Omega q\, \mathrm{div}\, \boldsymbol{u} = 0,$$

for all $(\boldsymbol{v}, \boldsymbol{\theta}, q) \in \mathrm{H}_0^1(\Omega)^d \times \mathrm{L}^2(\Omega)^{d(d-1)/2} \times \mathrm{L}_0^2(\Omega)$, where $\mathrm{L}_0^2(\Omega) := \{q \in \mathrm{L}^2(\Omega) : (q,1)_{0,\Omega} = 0\}$.

Contrary to what is usually found in the the standard velocity-pressure mixed formulation, the ellipticity on the kernel condition for the Babuška-Brezzi theory is not straightforward in the above mixed formulation. Here is where the augmentation contributes to simplify the analysis. We introduce the following residual terms arising from equations (2.5b) and (2.5c):

$$\kappa_1 \int_\Omega (\mathbf{curl}\, \boldsymbol{u} - \boldsymbol{\omega}) \cdot \mathbf{curl}\, \boldsymbol{v} = 0, \qquad \kappa_2 \int_\Omega \mathrm{div}\, \boldsymbol{u}\, \mathrm{div}\, \boldsymbol{v} = 0 \qquad \forall \boldsymbol{v} \in \mathrm{H}_0^1(\Omega)^d,$$

where κ_1 and κ_2 are positive parameters to be specified later on.

In this way, we propose the following augmented variational formulation for (2.5):

Find $((\boldsymbol{u}, \boldsymbol{\omega}), p) \in (\mathrm{H}_0^1(\Omega)^d \times \mathrm{L}^2(\Omega)^{d(d-1)/2}) \times \mathrm{L}_0^2(\Omega)$ *such that*

$$A((\boldsymbol{u}, \boldsymbol{\omega}), (\boldsymbol{v}, \boldsymbol{\theta})) + B((\boldsymbol{v}, \boldsymbol{\theta}), p) = F(\boldsymbol{v}, \boldsymbol{\theta}) \qquad \forall (\boldsymbol{v}, \boldsymbol{\theta}) \in \mathrm{H}_0^1(\Omega)^d \times \mathrm{L}^2(\Omega)^{d(d-1)/2}, \tag{2.8a}$$

$$B((\boldsymbol{u}, \boldsymbol{\omega}), q) = 0 \qquad \forall q \in \mathrm{L}_0^2(\Omega), \tag{2.8b}$$

where the bilinear forms and the linear functional are defined by

$$A((\boldsymbol{u}, \boldsymbol{\omega}), (\boldsymbol{v}, \boldsymbol{\theta})) := \int_\Omega (\sigma\boldsymbol{u} + (\boldsymbol{\beta} \cdot \nabla)\boldsymbol{u}) \cdot \boldsymbol{v} + \int_\Omega \nu\boldsymbol{\omega} \cdot \boldsymbol{\theta} + \int_\Omega \nu\boldsymbol{\omega} \cdot \mathbf{curl}\, \boldsymbol{v} - \int_\Omega \nu\boldsymbol{\theta} \cdot \mathbf{curl}\, \boldsymbol{u}$$

$$+ \kappa_1 \int_\Omega \mathbf{curl}\, \boldsymbol{u} \cdot \mathbf{curl}\, \boldsymbol{v} + \kappa_2 \int_\Omega \mathrm{div}\, \boldsymbol{u}\, \mathrm{div}\, \boldsymbol{v} - \kappa_1 \int_\Omega \boldsymbol{\omega} \cdot \mathbf{curl}\, \boldsymbol{v}$$

$$- 2 \int_\Omega \boldsymbol{\varepsilon}(\boldsymbol{u})\nabla\nu \cdot \boldsymbol{v} + \int_\Omega \boldsymbol{\omega} \cdot (\nabla\nu \times \boldsymbol{v}), \tag{2.9a}$$

$$B((\boldsymbol{v}, \boldsymbol{\theta}), q) := - \int_\Omega q\, \mathrm{div}\, \boldsymbol{v}, \tag{2.9b}$$

$$F(\boldsymbol{v}, \boldsymbol{\theta}) := \int_\Omega \boldsymbol{f} \cdot \boldsymbol{v}, \tag{2.9c}$$

for all $(\boldsymbol{u}, \boldsymbol{\omega}), (\boldsymbol{v}, \boldsymbol{\theta}) \in \mathrm{H}_0^1(\Omega)^d \times \mathrm{L}^2(\Omega)^{d(d-1)/2}$, and $q \in \mathrm{L}_0^2(\Omega)$.

As we will address in full detail in the next section, the augmented mixed formulation will permit us to analyse the problem directly under the classical Babuška-Brezzi theory [16].

2.2. Well-posedness analysis. In this section, we will address the well-posedness of the proposed weak formulation (2.8).

In our analysis, we will need to invoke the following inequality, which is a consequence of the Sobolev embedding $\mathrm{H}^1(\Omega) \hookrightarrow \mathrm{L}^4(\Omega)$

$$\left| \int_\Omega \mathrm{div}\, \boldsymbol{\beta}(\boldsymbol{u} \cdot \boldsymbol{v}) \right| \leq \widehat{C} \|\mathrm{div}\, \boldsymbol{\beta}\|_{0,\Omega} \|\boldsymbol{u}\|_{1,\Omega} \|\boldsymbol{v}\|_{1,\Omega}. \tag{2.10}$$

We will also make use of the following identity (cf. [35, Lemma 2.2])

$$\int_\Omega [(\boldsymbol{\beta} \cdot \nabla)\boldsymbol{u}] \cdot \boldsymbol{v} + \int_\Omega [(\boldsymbol{\beta} \cdot \nabla)\boldsymbol{v}] \cdot \boldsymbol{u} = - \int_\Omega \operatorname{div} \boldsymbol{\beta}(\boldsymbol{u} \cdot \boldsymbol{v}). \tag{2.11}$$

The continuity of the bilinear forms and the linear functional (cf. (2.9a)-(2.9c)), will be a consequence of the following lemma, whose proof follows standard arguments in combination with (1.2).

LEMMA 2.1. *The following estimates hold*

$$\left| \sigma \int_\Omega \boldsymbol{u} \cdot \boldsymbol{v} \right| \le \sigma \|\boldsymbol{u}\|_{0,\Omega} \|\boldsymbol{v}\|_{0,\Omega}, \qquad \left| \int_\Omega \nu \boldsymbol{\omega} \cdot \boldsymbol{\theta} \right| \le \nu_1 \|\boldsymbol{\omega}\|_{0,\Omega} \|\boldsymbol{\theta}\|_{0,\Omega},$$

$$\left| \int_\Omega [(\boldsymbol{\beta} \cdot \nabla)\boldsymbol{u}] \cdot \boldsymbol{v} \right| \le \widehat{C} \|\boldsymbol{\beta}\|_{1,\Omega} \|\nabla \boldsymbol{u}\|_{0,\Omega} \|\boldsymbol{v}\|_{1,\Omega},$$

$$\left| \int_\Omega \nu \boldsymbol{\theta} \cdot \mathbf{curl}\, \boldsymbol{v} \right| \le \nu_1 \|\boldsymbol{\theta}\|_{0,\Omega} \|\boldsymbol{v}\|_{1,\Omega}, \qquad \left| \int_\Omega \boldsymbol{\varepsilon}(\boldsymbol{u}) \nabla \nu \cdot \boldsymbol{v} \right| \le \|\nabla \nu\|_{\infty,\Omega} \|\boldsymbol{\varepsilon}(\boldsymbol{u})\|_{0,\Omega} \|\boldsymbol{v}\|_{0,\Omega},$$

$$\left| \int_\Omega \boldsymbol{\theta} \cdot (\nabla \nu \times \boldsymbol{v}) \right| \le 2 \|\nabla \nu\|_{\infty,\Omega} \|\boldsymbol{v}\|_{0,\Omega} \|\boldsymbol{\theta}\|_{0,\Omega}, \qquad |F(\boldsymbol{v}, \boldsymbol{\theta})| \le \|\boldsymbol{f}\|_{0,\Omega} \|\boldsymbol{v}\|_{0,\Omega}.$$

As a consequence of the above lemma, there exist constants $C_1, C_2, C_3 > 0$ such that

$$|A((\boldsymbol{u}, \boldsymbol{\omega}), (\boldsymbol{v}, \boldsymbol{\theta}))| \le C_1 \|(\boldsymbol{u}, \boldsymbol{\omega})\| \|(\boldsymbol{v}, \boldsymbol{\theta})\|, \qquad |B((\boldsymbol{v}, \boldsymbol{\theta}), q)| \le C_2 \|(\boldsymbol{v}, \boldsymbol{\theta})\| \|q\|_{0,\Omega},$$
$$|F(\boldsymbol{v}, \boldsymbol{\theta})| \le C_3 \|(\boldsymbol{v}, \boldsymbol{\theta})\|,$$

with the product space norm defined as

$$\|(\boldsymbol{v}, \boldsymbol{\theta})\|^2 := \|\boldsymbol{v}\|_{1,\Omega}^2 + \|\boldsymbol{\theta}\|_{0,\Omega}^2.$$

The following lemma states the ellipticity of the bilinear form $A(\cdot, \cdot)$.

LEMMA 2.2. *Assume that*

$$\sigma > \frac{9\|\nabla \nu\|_{\infty,\Omega}^2}{\nu_0} \quad and \quad \widehat{C} \|\operatorname{div} \boldsymbol{\beta}\|_{0,\Omega} < \min\left\{ \sigma - \frac{9\|\nabla \nu\|_{\infty,\Omega}^2}{\nu_0}, \frac{\nu_0}{12} \right\}. \tag{2.12}$$

Then, if we choose $\kappa_1 = \frac{2}{3}\nu_0$ *and* $\kappa_2 > \dfrac{\nu_0}{3}$, *there exists a constant* $\alpha > 0$ *such that*

$$A((\boldsymbol{v}, \boldsymbol{\theta}), (\boldsymbol{v}, \boldsymbol{\theta})) \ge \alpha \|(\boldsymbol{v}, \boldsymbol{\theta})\|^2 \qquad \forall (\boldsymbol{v}, \boldsymbol{\theta}) \in \mathrm{H}_0^1(\Omega)^d \times \mathrm{L}^2(\Omega)^{d(d-1)/2}.$$

Proof. Let $(\boldsymbol{v}, \boldsymbol{\theta}) \in \mathrm{H}_0^1(\Omega)^d \times \mathrm{L}^2(\Omega)^{d(d-1)/2}$. As a consequence of Lemma 2.1, we have that

$$\left| 2 \int_\Omega \boldsymbol{\varepsilon}(\boldsymbol{v}) \nabla \nu \cdot \boldsymbol{v} \right| \le 2\|\nabla \nu\|_{\infty,\Omega} \left(\frac{\nu_0}{12\|\nabla \nu\|_{\infty,\Omega}} \|\nabla \boldsymbol{v}\|_{0,\Omega}^2 + \frac{3\|\nabla \nu\|_{\infty,\Omega}}{\nu_0} \|\boldsymbol{v}\|_{0,\Omega}^2 \right)$$

$$= \frac{\nu_0}{6}(\|\mathbf{curl}\, \boldsymbol{v}\|_{0,\Omega}^2 + \|\operatorname{div} \boldsymbol{v}\|_{0,\Omega}^2) + \frac{6\|\nabla \nu\|_{\infty,\Omega}^2}{\nu_0} \|\boldsymbol{v}\|_{0,\Omega}^2, \tag{2.13}$$

where we have used (2.6). Moreover, using that $\|(\nabla \nu \times \boldsymbol{v})\|_{0,\Omega} \le 2\|\nabla \nu\|_{\infty,\Omega} \|\boldsymbol{v}\|_{0,\Omega}$, we get

$$\left| \int_\Omega \boldsymbol{\theta} \cdot (\nabla \nu \times \boldsymbol{v}) \right| \le 2\|\nabla \nu\|_{\infty,\Omega} \left(\frac{\nu_0}{6\|\nabla \nu\|_{\infty,\Omega}} \|\boldsymbol{\theta}\|_{0,\Omega}^2 + \frac{3\|\nabla \nu\|_{\infty,\Omega}}{2\nu_0} \|\boldsymbol{v}\|_{0,\Omega}^2 \right)$$

$$= \frac{\nu_0}{3} \|\boldsymbol{\theta}\|_{0,\Omega}^2 + \frac{3\|\nabla \nu\|_{\infty,\Omega}^2}{\nu_0} \|\boldsymbol{v}\|_{0,\Omega}^2,$$

$$\left| \kappa_1 \int_\Omega \boldsymbol{\theta} \cdot \mathbf{curl}\, \boldsymbol{v} \right| \le \kappa_1 \left(\frac{\nu_0}{3\kappa_1} \|\boldsymbol{\theta}\|_{0,\Omega}^2 + \frac{3\kappa_1}{4\nu_0} \|\mathbf{curl}\, \boldsymbol{v}\|_{0,\Omega}^2 \right)$$

$$= \frac{\nu_0}{3}\|\boldsymbol{\theta}\|_{0,\Omega}^2 + \frac{3\kappa_1^2}{4\nu_0}\|\operatorname{\mathbf{curl}} v\|_{0,\Omega}^2. \tag{2.14}$$

Thus, using the Cauchy-Schwarz inequality, (2.13)-(2.14), (2.11) and (2.10), we obtain

$$\begin{aligned}
A((\boldsymbol{v},\boldsymbol{\theta}),(\boldsymbol{v},\boldsymbol{\theta})) \geq &\sigma\|\boldsymbol{v}\|_{0,\Omega}^2 + \int_\Omega [(\boldsymbol{\beta}\cdot\nabla)\boldsymbol{v}]\cdot\boldsymbol{v} + \int_\Omega \nu|\boldsymbol{\theta}|^2 + \kappa_1\|\operatorname{\mathbf{curl}} v\|_{0,\Omega}^2 + \kappa_2\|\operatorname{div} v\|_{0,\Omega}^2 \\
&- \kappa_1\int_\Omega \boldsymbol{\theta}\cdot\operatorname{\mathbf{curl}} v - 2\int_\Omega \boldsymbol{\varepsilon}(\boldsymbol{v})\nabla\nu\cdot\boldsymbol{v} + \int_\Omega \boldsymbol{\theta}\cdot(\nabla\nu\times\boldsymbol{v}) \\
\geq &\sigma\|\boldsymbol{v}\|_{0,\Omega}^2 - \widehat{C}\|\operatorname{div}\boldsymbol{\beta}\|_{0,\Omega}\|\boldsymbol{v}\|_{1,\Omega}^2 + \nu_0\|\boldsymbol{\theta}\|_{0,\Omega}^2 + \kappa_1\|\operatorname{\mathbf{curl}} v\|_{0,\Omega}^2 + \kappa_2\|\operatorname{div} v\|_{0,\Omega}^2 \\
&- \frac{\nu_0}{3}\|\boldsymbol{\theta}\|_{0,\Omega}^2 - \frac{3\kappa_1^2}{4\nu_0}\|\operatorname{\mathbf{curl}} v\|_{0,\Omega}^2 - \frac{\nu_0}{6}(\|\operatorname{\mathbf{curl}} v\|_{0,\Omega}^2 + \|\operatorname{div} v\|_{0,\Omega}^2) \\
&- \frac{6\|\nabla\nu\|_{\infty,\Omega}^2}{\nu_0}\|\boldsymbol{v}\|_{0,\Omega}^2 - \frac{\nu_0}{3}\|\boldsymbol{\theta}\|_{0,\Omega}^2 - \frac{3\|\nabla\nu\|_{\infty,\Omega}^2}{\nu_0}\|\boldsymbol{v}\|_{0,\Omega}^2 \\
= &\frac{\nu_0}{3}\|\boldsymbol{\theta}\|_{0,\Omega}^2 + \left(\frac{\nu_0}{6} - \widehat{C}\|\operatorname{div}\boldsymbol{\beta}\|_{0,\Omega}\right)\|\operatorname{\mathbf{curl}} v\|_{0,\Omega}^2 \\
&+ \left(\kappa_2 - \frac{\nu_0}{6} - \widehat{C}\|\operatorname{div}\boldsymbol{\beta}\|_{0,\Omega}\right)\|\operatorname{div} v\|_{0,\Omega}^2 \\
&+ \left(\sigma - \frac{9\|\nabla\nu\|_{\infty,\Omega}^2}{\nu_0} - \widehat{C}\|\operatorname{div}\boldsymbol{\beta}\|_{0,\Omega}\right)\|\boldsymbol{v}\|_{0,\Omega}^2.
\end{aligned}$$

Now, using assumption (2.12), we have

$$A((\boldsymbol{v},\boldsymbol{\theta}),(\boldsymbol{v},\boldsymbol{\theta})) \geq \alpha\|(\boldsymbol{v},\boldsymbol{\theta})\|^2,$$

where

$$\alpha := \min\left\{\frac{\nu_0}{3}, \frac{\nu_0}{6} - \widehat{C}\|\operatorname{div}\boldsymbol{\beta}\|_{0,\Omega}, \kappa_2 - \frac{\nu_0}{6} - \widehat{C}\|\operatorname{div}\boldsymbol{\beta}\|_{0,\Omega}, \sigma - \frac{9\|\nabla\nu\|_{0,\Omega}^2}{\nu_0} - \widehat{C}\|\operatorname{div}\boldsymbol{\beta}\|_{0,\Omega}\right\},$$

which is clearly positive according to (2.12) and the assumptions on κ_1 and κ_2. □

Now we recall the following result related to the inf-sup condition: There exists $C > 0$, depending only on Ω, such that (cf. [33])

$$\sup_{0\neq\boldsymbol{v}\in\mathrm{H}_0^1(\Omega)^d} \frac{\left|\int_\Omega q\operatorname{div}\boldsymbol{v}\right|}{\|\boldsymbol{v}\|_{1,\Omega}} \geq C\|q\|_{0,\Omega} \quad \forall q\in\mathrm{L}_0^2(\Omega).$$

As a consequence, we immediately have the following lemma.

LEMMA 2.3. *There exists $\gamma > 0$, independent of ν, such that*

$$\sup_{0\neq(\boldsymbol{v},\boldsymbol{\theta})\in\mathrm{H}_0^1(\Omega)^d\times\mathrm{L}^2(\Omega)^{d(d-1)/2}} \frac{|B((\boldsymbol{v},\boldsymbol{\theta}),q)|}{\|(\boldsymbol{v},\boldsymbol{\theta})\|} \geq \gamma\|q\|_{0,\Omega} \quad \forall q\in\mathrm{L}_0^2(\Omega).$$

We state the well-posedness of problem (2.8) in the next theorem.

THEOREM 2.4. *Assume that the hypotheses of Lemma 2.2 hold true. Then, there exists a unique solution $((\boldsymbol{u},\boldsymbol{\omega}),p) \in (\mathrm{H}_0^1(\Omega)^d\times\mathrm{L}^2(\Omega)^{d(d-1)/2})\times\mathrm{L}_0^2(\Omega)$ to problem (2.8). Moreover, there exists $C > 0$ such that*

$$\|(\boldsymbol{u},\boldsymbol{\omega})\| + \|p\|_{0,\Omega} \leq C\|\boldsymbol{f}\|_{0,\Omega}.$$

Proof. The proof follows from Lemmas 2.2 and 2.3, and a direct consequence of the Babuška-Brezzi Theorem ([16, Theorem II.1.1]). □

REMARK 2.5. *The unique solution of problem (2.8) also solves (2.5a)-(2.5e). The equivalence follows essentially from applying integration by parts backwardly in (2.8) and using suitable test functions. This is employed in Section 4 to prove the efficiency of the a posteriori error estimator.*

REMARK 2.6. *If the convective velocity $\boldsymbol{\beta} \in \mathrm{H}^1(\Omega)^d$ is solenoidal (i.e., $\operatorname{div} \boldsymbol{\beta} = 0$ in Ω), then problem (2.8) is well-posed after choosing $\kappa_1 = \frac{2}{3}\nu_0$, $\kappa_2 > \dfrac{\nu_0}{3}$, and assuming*

$$\sigma\nu_0 > 9\|\nabla\nu\|^2_{\infty,\Omega}. \tag{2.15}$$

3. Numerical discretisation. Let $\{\mathcal{T}_h(\Omega)\}_{h>0}$ be a shape-regular family of partitions of the polygonal/polyhedral region $\bar{\Omega}$, by triangles/tetrahedrons T of diameter h_T, with the meshsize defined as $h := \max\{h_T : T \in \mathcal{T}_h(\Omega)\}$. In what follows, given an integer $k \geq 0$ and a subset S of $\mathbb{R}^d$, $\mathbb{P}_k(S)$ denotes the space of polynomial functions defined on S and being of degree $\leq k$.

Now, we consider generic finite dimensional subspaces $\mathbf{V}_h \subseteq \mathrm{H}^1_0(\Omega)^d$, $\mathbf{W}_h \subseteq \mathrm{L}^2(\Omega)^{d(d-1)/2}$ and $Q_h \subseteq \mathrm{L}^2_0(\Omega)$ such that the following discrete inf-sup holds

$$\sup_{0 \neq (\boldsymbol{v}_h, \boldsymbol{\theta}_h) \in \mathbf{V}_h \times \mathbf{W}_h} \frac{|B((\boldsymbol{v}_h, \boldsymbol{\theta}_h), q_h)|}{\|(\boldsymbol{v}_h, \boldsymbol{\theta}_h)\|} \geq \gamma_0 \|q_h\|_{0,\Omega} \quad \forall q_h \in Q_h, \tag{3.16}$$

where $\gamma_0 > 0$ is independent of h.

In this way, the above inf-sup condition can be obtained if $(\mathbf{V}_h, Q_h)$ is an inf-sup stable pair for the classical Stokes problem. Moreover, the discrete space $\mathbf{W}_h \subseteq \mathrm{L}^2(\Omega)^{d(d-1)/2}$ for the vorticity can be taken as continuous or discontinuous polynomial space. Here we will consider both options.

Now, we are in a position to introduce the finite element scheme related to problem (2.8): Find $((\boldsymbol{u}_h, \boldsymbol{\omega}_h), p_h) \in (\mathbf{V}_h \times \mathbf{W}_h) \times Q_h$ such that

$$
\begin{aligned}
A((\boldsymbol{u}_h, \boldsymbol{\omega}_h), (\boldsymbol{v}_h, \boldsymbol{\theta}_h)) + B((\boldsymbol{v}_h, \boldsymbol{\theta}_h), p_h) &= F(\boldsymbol{v}_h, \boldsymbol{\theta}_h) &&\forall (\boldsymbol{v}_h, \boldsymbol{\theta}_h) \in \mathbf{V}_h \times \mathbf{W}_h, \\
B((\boldsymbol{u}_h, \boldsymbol{\omega}_h), q_h) &= 0 &&\forall q \in Q_h.
\end{aligned} \tag{3.17}
$$

The next step is to establish the unique solvability and convergence of the discrete problem (3.17).

THEOREM 3.1. *Assume that the hypotheses of Lemma 2.2 hold true. Let $\mathbf{V}_h \subseteq \mathrm{H}^1_0(\Omega)^d$, $\mathbf{W}_h \subseteq \mathrm{L}^2(\Omega)^{d(d-1)/2}$ and $Q_h \subseteq \mathrm{L}^2_0(\Omega)$ satisfy (3.16). Then, there exists a unique $((\boldsymbol{u}_h, \boldsymbol{\omega}_h), p_h) \in (\mathbf{V}_h \times \mathbf{W}_h) \times Q_h$ solution to (3.17). Moreover, there exist $\hat{C}_1, \hat{C}_2 > 0$, independent of h, such that*

$$\|(\boldsymbol{u}_h, \boldsymbol{\omega}_h)\| + \|p_h\|_{0,\Omega} \leq \hat{C}_1\|\boldsymbol{f}\|_{0,\Omega},$$

and

$$
\begin{aligned}
\|(\boldsymbol{u}, \boldsymbol{\omega}) &- (\boldsymbol{u}_h, \boldsymbol{\omega}_h)\| + \|p - p_h\|_{0,\Omega} \\
&\leq \hat{C}_2 \inf_{(\boldsymbol{v}_h, \boldsymbol{\theta}_h, q_h) \in \mathbf{V}_h \times \mathbf{W}_h \times \mathrm{Q}_h} (\|\boldsymbol{u} - \boldsymbol{v}_h\|_{1,\Omega} + \|\boldsymbol{\omega} - \boldsymbol{\theta}_h\|_{0,\Omega} + \|p - q_h\|_{0,\Omega}),
\end{aligned} \tag{3.18}
$$

where $((\boldsymbol{u}, \boldsymbol{\omega}), p) \in (\mathrm{H}^1_0(\Omega)^d \times \mathrm{L}^2(\Omega)^{d(d-1)/2}) \times \mathrm{L}^2_0(\Omega)$ is the unique solution of (2.8).

3.1. Discrete subspaces and error estimates. In this section, we will define explicit families of finite element subspaces yielding the unique solvability of the discrete scheme (3.17). In addition, we derive the corresponding rate of convergence for each family.

3.1.1. Taylor-Hood-$\mathbb{P}_k$. We start by introducing a family based on Taylor-Hood [36] finite elements for velocity and pressure, and continuous or discontinuous piecewise polynomial spaces for vorticity. More precisely, for any $k \geq 1$, we consider:

$$
\begin{aligned}
\mathbf{V}_h &:= \{\boldsymbol{v}_h \in C(\overline{\Omega})^d : \boldsymbol{v}_h|_K \in \mathbb{P}_{k+1}(K)^d \quad \forall K \in \mathcal{T}_h\} \cap \mathrm{H}^1_0(\Omega)^d, \\
Q_h &:= \{q_h \in C(\overline{\Omega}) : q_h|_K \in \mathbb{P}_k(K) \quad \forall K \in \mathcal{T}_h\} \cap \mathrm{L}^2_0(\Omega), \\
\mathbf{W}^1_h &:= \{\boldsymbol{\theta}_h \in C(\overline{\Omega})^{d(d-1)/2} : \boldsymbol{\theta}_h|_K \in \mathbb{P}_k(K)^{d(d-1)/2} \quad \forall K \in \mathcal{T}_h\}, \\
\mathbf{W}^2_h &:= \{\boldsymbol{\theta}_h \in \mathrm{L}^2(\Omega)^{d(d-1)/2} : \boldsymbol{\theta}_h|_K \in \mathbb{P}_k(K)^{d(d-1)/2} \quad \forall K \in \mathcal{T}_h\}.
\end{aligned} \tag{3.19}
$$

It is well known that $(\mathbf{V}_h, Q_h)$ satisfies the inf-sup condition (3.16) [15]. In addition, we will consider continuous ($\mathbf{W}^1_h$) and discontinuous ($\mathbf{W}^2_h$) polynomial approximations for vorticity.

Now, we recall the approximation properties of the spaces specified in (3.19). Assume that $\boldsymbol{u} \in \mathrm{H}^{1+s}(\Omega)^d$, $p \in \mathrm{H}^s(\Omega)$ and $\boldsymbol{\omega} \in \mathrm{H}^s(\Omega)^{d(d-1)/2}$, for some $s \in (1/2, k+1]$. Then there exists $C > 0$, independent of h, such that

$$\inf_{\boldsymbol{v}_h \in \mathbf{V}_h} \|\boldsymbol{u} - \boldsymbol{v}_h\|_{1,\Omega} \leq C h^s \|\boldsymbol{u}\|_{\mathrm{H}^{1+s}(\Omega)^d}, \tag{3.20a}$$

$$\inf_{q_h \in Q_h} \|p - q_h\|_{0,\Omega} \leq C h^s \|p\|_{\mathrm{H}^s(\Omega)}, \tag{3.20b}$$

$$\inf_{\boldsymbol{\theta}_h \in \mathbf{W}_h^1} \|\boldsymbol{\omega} - \boldsymbol{\theta}_h\|_{0,\Omega} \leq C h^s \|\boldsymbol{\omega}\|_{\mathrm{H}^s(\Omega)^{d(d-1)/2}}, \tag{3.20c}$$

$$\inf_{\boldsymbol{\theta}_h \in \mathbf{W}_h^2} \|\boldsymbol{\omega} - \boldsymbol{\theta}_h\|_{0,\Omega} \leq C h^s \|\boldsymbol{\omega}\|_{\mathrm{H}^s(\Omega)^{d(d-1)/2}}. \tag{3.20d}$$

The following theorem provides the rate of convergence of the augmented mixed scheme (3.17).

THEOREM 3.2. *Let $k \geq 1$ be an integer, and let $\mathbf{V}_h, Q_h$ and W_h^i, $i = 1, 2$ be specified by (3.19). Let $(\boldsymbol{u}, \boldsymbol{\omega}, p) \in \mathrm{H}_0^1(\Omega)^d \times \mathrm{L}^2(\Omega)^{d(d-1)/2} \times \mathrm{L}_0^2(\Omega)$ and $(\boldsymbol{u}_h, \boldsymbol{\omega}_h, p_h) \in \mathbf{V}_h \times \mathbf{W}_h^i \times Q_h$ be the unique solutions to the continuous and discrete problems (2.8) and (3.17), respectively. Assume that $\boldsymbol{u} \in \mathrm{H}^{1+s}(\Omega)^d$, $\boldsymbol{\omega} \in \mathrm{H}^s(\Omega)^{d(d-1)/2}$ and $p \in \mathrm{H}^s(\Omega)$, for some $s \in (1/2, k+1]$. Then, there exists $\hat{C} > 0$, independent of h, such that*

$$\|(\boldsymbol{u}, \boldsymbol{\omega}) - (\boldsymbol{u}_h, \boldsymbol{\omega}_h)\| + \|p - p_h\|_{0,\Omega} \leq \hat{C} h^s (\|\boldsymbol{u}\|_{\mathrm{H}^{1+s}(\Omega)^d} + \|\boldsymbol{\omega}\|_{\mathrm{H}^s(\Omega)^{d(d-1)/2}} + \|p\|_{\mathrm{H}^s(\Omega)}).$$

Proof. The proof follows from (3.18) and the approximation properties (3.20a)-(3.20d). ☐

3.1.2. MINI-element-$\mathbb{P}_k$. The second finite element family uses the so-called MINI-element for velocity and pressure, and continuous or discontinuous piecewise polynomials for vorticity. Let us introduce the following spaces (see [16, Sections 8.6 and 8.7], for further details):

$$\mathbf{U}_h := \{\boldsymbol{v}_h \in C(\overline{\Omega})^d : \boldsymbol{v}_h|_K \in \mathbb{P}_k(K)^d \quad \forall K \in \mathcal{T}_h\},$$

$$\mathbb{B}(b_K \nabla H_h) := \{\boldsymbol{v}_{hb} \in \mathrm{H}^1(\Omega)^d : \boldsymbol{v}_{hb}|_K = b_K \nabla(q_h)|_K \text{ for some } q_h \in H_h\},$$

where b_K is the standard (cubic or quartic) bubble function $\lambda_1 \cdots \lambda_{d+1} \in \mathbb{P}_{d+1}(K)$, and let us define the following finite element subspaces:

$$\begin{aligned} Q_h &:= \{q_h \in C(\overline{\Omega}) : q_h|_K \in \mathbb{P}_k(K) \quad \forall K \in \mathcal{T}_h\} \cap \mathrm{L}_0^2(\Omega), \\ \mathbf{V}_h &:= \mathbf{U}_h \oplus \mathbb{B}(b_K \nabla Q_h) \cap \mathrm{H}_0^1(\Omega)^d, \\ \mathbf{W}_h^1 &:= \{\boldsymbol{\theta}_h \in C(\overline{\Omega})^{d(d-1)/2} : \boldsymbol{\theta}_h|_K \in \mathbb{P}_k(K)^{d(d-1)/2} \quad \forall K \in \mathcal{T}_h\}, \\ \mathbf{W}_h^2 &:= \{\boldsymbol{\theta}_h \in \mathrm{L}^2(\Omega)^{d(d-1)/2} : \boldsymbol{\theta}_h|_K \in \mathbb{P}_k(K)^{d(d-1)/2} \quad \forall K \in \mathcal{T}_h\}. \end{aligned} \tag{3.21}$$

The rate of convergence of our augmented mixed finite element scheme considering the above discrete spaces (3.21) is as follows.

THEOREM 3.3. *Let $k \geq 1$ be an integer, and let $\mathbf{V}_h, Q_h$ and W_h^i, $i = 1, 2$ be given by (3.21). Let $(\boldsymbol{u}, \boldsymbol{\omega}, p) \in \mathrm{H}_0^1(\Omega)^d \times \mathrm{L}^2(\Omega)^{d(d-1)/2} \times \mathrm{L}_0^2(\Omega)$ and $(\boldsymbol{u}_h, \boldsymbol{\omega}_h, p_h) \in \mathbf{V}_h \times \mathbf{W}_h^i \times Q_h$ be the unique solutions to the continuous and discrete problems (2.8) and (3.17), respectively. Assume that $\boldsymbol{u} \in \mathrm{H}^{1+s}(\Omega)^d$, $\boldsymbol{\omega} \in \mathrm{H}^s(\Omega)^{d(d-1)/2}$ and $p \in \mathrm{H}^s(\Omega)$, for some $s \in (1/2, k]$. Then, there exists $\hat{C} > 0$, independent of h, such that*

$$\|(\boldsymbol{u}, \boldsymbol{\omega}) - (\boldsymbol{u}_h, \boldsymbol{\omega}_h)\| + \|p - p_h\|_{0,\Omega} \leq \hat{C} h^s (\|\boldsymbol{u}\|_{\mathrm{H}^{1+s}(\Omega)^d} + \|\boldsymbol{\omega}\|_{\mathrm{H}^s(\Omega)^{d(d-1)/2}} + \|p\|_{\mathrm{H}^s(\Omega)}).$$

4. A posteriori error estimator. In this section, we propose a residual-based a posteriori error estimator and prove its reliability and efficiency. The analysis restricts to the two-dimensional case and using continuous finite element approximations for vorticity. Nevertheless, the extension to 3D and to discontinuous vorticity follows straightforwardly.

For each $T \in \mathcal{T}_h$ we let $\mathcal{E}(T)$ be the set of edges of T, and we denote by $\mathcal{E}_h$ the set of all edges in $\mathcal{T}_h$, that is

$$\mathcal{E}_h = \mathcal{E}_h(\Omega) \cup \mathcal{E}_h(\Gamma),$$

where $\mathcal{E}_h(\Omega) := \{e \in \mathcal{E}_h : e \subset \Omega\}$, and $\mathcal{E}_h(\Gamma) := \{e \in \mathcal{E}_h : e \subset \Gamma\}$. In what follows, h_e stands for the diameter of a given edge $e \in \mathcal{E}_h$, $\boldsymbol{t}_e = (-n_2, n_1)$, where $\boldsymbol{n}_e = (n_1, n_2)$ is a fix unit normal vector of e. Now, let $q \in \mathrm{L}^2(\Omega)$ such that $q|_T \in C(T)$ for each $T \in \mathcal{T}_h$, then given $e \in \mathcal{E}_h(\Omega)$, we denote by $[q]$ the jump of q across e, that is $[q] := (q|_{T'})|_e - (q|_{T''})|_e$, where T' and T'' are the triangles of $\mathcal{T}_h$ sharing the edge e. Moreover, let $\boldsymbol{v} \in \mathrm{L}^2(\Omega)^2$ such that $\boldsymbol{v}|_T \in C(T)^2$ for each $T \in \mathcal{T}_h$. Then, given $e \in \mathcal{E}_h(\Omega)$, we denote by $[\boldsymbol{v} \cdot \boldsymbol{t}]$ the tangential jump of $\boldsymbol{v}$ across e, that is, $[\boldsymbol{v} \cdot \boldsymbol{t}] := ((\boldsymbol{v}|_{T'})|_e - (\boldsymbol{v}|_{T''})|_e) \cdot \boldsymbol{t}_e$, where T' and T'' are the triangles of $\mathcal{T}_h$ sharing the edge e.

Next, let $k \geq 1$ be an integer, and let $\mathbf{V}_h, Q_h$ and $\mathbf{W}_h^1$ be given as in (3.19) or (3.21). Let $(\boldsymbol{u}, \omega, p) \in \mathrm{H}_0^1(\Omega)^2 \times \mathrm{L}^2(\Omega) \times \mathrm{L}_0^2(\Omega)$ and $(\boldsymbol{u}_h, \omega_h, p_h) \in \mathbf{V}_h \times \mathbf{W}_h^1 \times Q_h$ be the unique solutions to the continuous and discrete problems (2.8) and (3.17), respectively. We introduce for each $T \in \mathcal{T}_h$ the local *a posteriori* error indicator and its global counterpart as

$$
\begin{aligned}
\Theta_T^2 :=& h_T^2 \| \boldsymbol{f} - \sigma \boldsymbol{u}_h - \nu \operatorname{\mathbf{curl}} \omega_h - (\boldsymbol{\beta} \cdot \nabla)\boldsymbol{u}_h + 2\boldsymbol{\varepsilon}(\boldsymbol{u}_h)\nabla\nu - \nabla p_h \|_{0,T}^2 \\
&+ \| \omega_h - \operatorname{\mathbf{curl}} \boldsymbol{u}_h \|_{0,T}^2 + \| \operatorname{div} \boldsymbol{u}_h \|_{0,T}^2, \qquad \Theta^2 := \sum_{T \in \mathcal{T}_h} \Theta_T^2.
\end{aligned}
\tag{4.22}
$$

Let us now establish reliability and efficiency of (4.22).

4.1. Reliability. We begin by recalling that the continuous dependence result given in Theorem 2.4 is equivalent to the global inf–sup condition for the continuous formulation (2.8). Then, applying this estimate to the error $(\boldsymbol{u} - \boldsymbol{u}_h, \omega - \omega_h, p - p_h)$, we obtain

$$
\|(\boldsymbol{u}, \omega) - (\boldsymbol{u}_h, \omega_h)\| + \|p - p_h\|_{0,\Omega} \leq C_{glob} \sup_{(\boldsymbol{v}_h, \theta_h, q_h) \in} \frac{\mathcal{R}(\boldsymbol{v}, \theta, q)}{\|(\boldsymbol{v}, \theta, q)\|},
\tag{4.23}
$$

where the residual functional $\mathcal{R}$ is defined by

$$
\mathcal{R}(\boldsymbol{v}, \theta, q) = A((\boldsymbol{u} - \boldsymbol{u}_h, \omega - \omega_h), (\boldsymbol{v}, \theta)) + B((\boldsymbol{v}, \theta), p - p_h) + B((\boldsymbol{u} - \boldsymbol{u}_h, \omega - \omega_h), q),
\tag{4.24}
$$

for all $(\boldsymbol{v}, \theta, q) \in \mathrm{H}_0^1(\Omega)^2 \times \mathrm{L}^2(\Omega) \times \mathrm{L}_0^2(\Omega)$.

Some technical results are provided beforehand. Let us first recall the Clément-type interpolation operator $\mathcal{I}_h : \mathrm{H}_0^1(\Omega) \to Y_h$, where $Y_h := \{v_h \in C(\overline{\Omega}) \cap \mathrm{H}_0^1(\Omega) : v_h|_T \in \mathbb{P}_1(T), \forall T \in \mathcal{T}_h\}$. This operator satisfies the following local approximation properties (cf. [22]).

LEMMA 4.1. *There exist positive constants C_1 and C_2 such that for all $v \in \mathrm{H}_0^1(\Omega)$ there hold*

$$
\|v - \mathcal{I}_h v\|_{0,T} \leq C_1 h_T |v|_{1,w_T} \quad \forall T \in \mathcal{T}_h,
\tag{4.25a}
$$

$$
\|v - \mathcal{I}_h v\|_{0,e} \leq C_2 h_e^{1/2} |v|_{1,w_e} \quad \forall e \in \mathcal{E}_h(\Omega),
\tag{4.25b}
$$

where $w_T := \bigcup\{T' \in \mathcal{T}_h : T' \cap T \neq \emptyset\}$ and $w_e := \bigcup\{T' \in \mathcal{T}_h : T' \cap e \neq \emptyset\}$.

The main result of this section is stated as follows.

THEOREM 4.2. *There exists a positive constant C_{rel}, independent of h, such that*

$$
\|(\boldsymbol{u}, \omega) - (\boldsymbol{u}_h, \omega_h)\| + \|p - p_h\|_{0,\Omega} \leq C_{\mathrm{rel}} \, \Theta.
\tag{4.26}
$$

Proof. From (4.24) and the continuous problem (2.8), we have that,

$$
\begin{aligned}
\mathcal{R}(\boldsymbol{v}, \theta, q) =& \int_\Omega \boldsymbol{f} \cdot \boldsymbol{v} - \Big(A((\boldsymbol{u}_h, \omega_h), (\boldsymbol{v}, \theta)) + B((\boldsymbol{v}, \theta), p_h) + B((\boldsymbol{u}_h, \omega_h), q) \Big) \\
=& \int_\Omega (\boldsymbol{f} - \sigma \boldsymbol{u}_h - (\boldsymbol{\beta} \cdot \nabla)\boldsymbol{u}_h + 2\boldsymbol{\varepsilon}(\boldsymbol{u}_h)\nabla\nu) \cdot \boldsymbol{v} - \int_\Omega \nu(\omega_h - \operatorname{\mathbf{curl}} \boldsymbol{u}_h)\theta \\
&- \kappa_1 \int_\Omega (\operatorname{\mathbf{curl}} \boldsymbol{u}_h - \omega_h) \operatorname{\mathbf{curl}} \boldsymbol{v} - \kappa_2 \int_\Omega \operatorname{div} \boldsymbol{u}_h \operatorname{div} \boldsymbol{v} \\
&- \left(\int_\Omega \nu \omega_h \operatorname{\mathbf{curl}} \boldsymbol{v} + \int_\Omega \omega_h (\nabla\nu \times \boldsymbol{v}) \right) + \int_\Omega p_h \operatorname{div} \boldsymbol{v} + \int_\Omega q \operatorname{div} \boldsymbol{u}_h.
\end{aligned}
$$

Using the identity $\mathbf{curl}(\nu \boldsymbol{v}) = \nabla \nu \times \boldsymbol{v} + \nu \, \mathbf{curl}\, \boldsymbol{v}$ and integration by parts on the above residual (cf. (1.4)), we obtain

$$
\begin{aligned}
\mathcal{R}(\boldsymbol{v}, \theta, q) = {} & \int_\Omega (\boldsymbol{f} - \sigma \boldsymbol{u}_h - (\boldsymbol{\beta} \cdot \nabla)\boldsymbol{u}_h + 2\varepsilon(\boldsymbol{u}_h)\nabla \nu) \cdot \boldsymbol{v} - \int_\Omega \nu(\omega_h - \mathbf{curl}\, \boldsymbol{u}_h)\theta \\
& - \kappa_1 \int_\Omega (\mathbf{curl}\, \boldsymbol{u}_h - \omega_h)\, \mathbf{curl}\, \boldsymbol{v} - \kappa_2 \int_\Omega \operatorname{div} \boldsymbol{u}_h \operatorname{div} \boldsymbol{v} + \int_\Omega q \operatorname{div} \boldsymbol{u}_h \\
& - \sum_{T \in \mathcal{T}_h} \left(\int_T \nu\, \mathbf{curl}\, \omega_h \cdot \boldsymbol{v} - \langle \boldsymbol{v} \cdot \boldsymbol{t}, \nu\omega_h \rangle_{\partial T} - \int_T \nabla p_h \cdot \boldsymbol{v} + \langle \boldsymbol{v} \cdot \boldsymbol{n}, p_h \rangle_{\partial T} \right) \\
= {} & \sum_{T \in \mathcal{T}_h} \int_T (\boldsymbol{f} - \sigma \boldsymbol{u}_h - \nu\, \mathbf{curl}\, \omega_h - (\boldsymbol{\beta} \cdot \nabla)\boldsymbol{u}_h + 2\varepsilon(\boldsymbol{u}_h)\nabla \nu - \nabla p_h) \cdot \boldsymbol{v} \\
& - \int_\Omega \nu(\omega_h - \mathbf{curl}\, \boldsymbol{u}_h)\theta - \kappa_1 \int_\Omega (\mathbf{curl}\, \boldsymbol{u}_h - \omega_h)\, \mathbf{curl}\, \boldsymbol{v} - \kappa_2 \int_\Omega \operatorname{div} \boldsymbol{u}_h \operatorname{div} \boldsymbol{v} + \int_\Omega q \operatorname{div} \boldsymbol{u}_h,
\end{aligned}
$$

where we have used the fact that ω_h and p_h are piecewise continuous functions. Hence, since from (4.24) we have $\mathcal{R}(\boldsymbol{v}_h, \theta_h, q_h) = 0$, we obtain

$$
\begin{aligned}
\mathcal{R}(\boldsymbol{v}, \theta, q) = {} & \mathcal{R}(\boldsymbol{v} - \boldsymbol{v}_h, \theta - \theta_h, q - q_h) \\
= {} & \sum_{T \in \mathcal{T}_h} \int_T \left(\boldsymbol{f} - \sigma \boldsymbol{u}_h - \nu\, \mathbf{curl}\, \omega_h - (\boldsymbol{\beta} \cdot \nabla)\boldsymbol{u}_h + 2\varepsilon(\boldsymbol{u}_h)\nabla \nu - \nabla p_h \right) \cdot (\boldsymbol{v} - \boldsymbol{v}_h) \\
& - \int_\Omega \nu(\omega_h - \mathbf{curl}\, \boldsymbol{u}_h)(\theta - \theta_h) - \kappa_1 \int_\Omega (\mathbf{curl}\, \boldsymbol{u}_h - \omega_h)\, \mathbf{curl}(\boldsymbol{v} - \boldsymbol{v}_h) \\
& - \kappa_2 \int_\Omega \operatorname{div} \boldsymbol{u}_h \operatorname{div}(\boldsymbol{v} - \boldsymbol{v}_h) + \int_\Omega (q - q_h) \operatorname{div} \boldsymbol{u}_h.
\end{aligned}
$$

Thus, it suffices to take $\boldsymbol{v}_h := \mathcal{I}_h(\boldsymbol{v})$ (cf. Lemma 4.1), and $\theta_h := \Pi(\theta)$ and $q_h := \Pi(q)$ with Π being the L^2-projection onto piecewise constants. And then, using the Cauchy-Schwarz inequality, triangle inequality, properties for $\mathcal{I}_h$ given by Lemma 4.1 and [28, Lemma 1.127], and approximation properties for Π, we obtain

$$
\begin{aligned}
\mathcal{R}(\boldsymbol{v}, \theta, q) \leq {} & C_1 \sum_{T \in \mathcal{T}_h} h_T \| \boldsymbol{f} - \sigma \boldsymbol{u}_h - \nu\, \mathbf{curl}\, \omega_h - (\boldsymbol{\beta} \cdot \nabla)\boldsymbol{u}_h + 2\varepsilon(\boldsymbol{u}_h)\nabla \nu - \nabla p_h \|_{0,T} |\boldsymbol{v}|_{1,w_T} \\
& + \sum_{T \in \mathcal{T}_h} (\nu_1 + \kappa_1)\| \omega_h - \mathbf{curl}\, \boldsymbol{u}_h \|_{0,T} (C_3 \|\theta\|_{0,T} + |\boldsymbol{v} - \boldsymbol{v}_h|_{1,T}) \\
& + \sum_{T \in \mathcal{T}_h} (\kappa_2 + 1)\| \operatorname{div} \boldsymbol{u}_h \|_{0,T} (|\boldsymbol{v} - \boldsymbol{v}_h|_{1,T} + C_4 \|q\|_{0,T}) \\
\leq {} & \widehat{C}_1 \left(\sum_{T \in \mathcal{T}_h} h_T^2 \| f - \sigma \boldsymbol{u}_h - \nu\, \mathbf{curl}\, \omega_h - (\boldsymbol{\beta} \cdot \nabla)\boldsymbol{u}_h + 2\varepsilon(\boldsymbol{u}_h)\nabla \nu - \nabla p_h \|_{0,T}^2 \right)^{1/2} \|\boldsymbol{v}\|_{1,\Omega} \\
& + \widehat{C}_2 \left(\sum_{T \in \mathcal{T}_h} \| \omega_h - \mathbf{curl}\, \boldsymbol{u}_h \|_{0,T}^2 \right)^{1/2} (\|\theta\|_{0,\Omega} + \|\boldsymbol{v}\|_{1,\Omega}) \\
& + \widehat{C}_3 \left(\sum_{T \in \mathcal{T}_h} \| \operatorname{div} \boldsymbol{u}_h \|_{0,T}^2 \right)^{1/2} (\|\boldsymbol{v}\|_{1,\Omega} + \|q\|_{0,\Omega}).
\end{aligned}
$$

And the proof of (4.26) follows from (4.23) and the above estimate. $\qquad\square$

4.2. Efficiency. This subsection deals with the efficiency of the *a posteriori* error estimator. For simplicity, we will assume that the given convective velocity $\boldsymbol{\beta}$ and the viscosity ν are polynomial functions both of degree s. The general case can be proved by repeating the same arguments and requiring an additional regularity for the data.

A major role in the proof of efficiency is played by element and edge bubbles (locally supported non-negative functions), whose definition we recall in what follows. For $T \in \mathcal{T}_h(\Omega)$ and $e \in \mathcal{E}(T)$, let ψ_T and ψ_e, respectively, be the interior and edge bubble functions defined as in, e.g., [1]. Let $\psi_T \in \mathbb{P}_3(T)$ with $supp(\psi_T) \subset T$, $\psi_T = 0$ on ∂T and $0 \leq \psi_T \leq 1$ in T. Moreover, let $\psi_e|_T \in \mathbb{P}_2(T)$ with $supp(\psi_e) \subset \Omega_e := \{T' \in \mathcal{T}_h(\Omega) : e \in \mathcal{E}(T')\}$, $\psi_e = 0$ on $\partial T \setminus e$, and $0 \leq \psi_e \leq 1$ in Ω_e. Again, let us recall an extension operator $E : C^0(e) \mapsto C^0(T)$ that satisfies $E(q) \in \mathbb{P}_k(T)$ and $E(q)|_e = q$ for all $q \in \mathbb{P}_k(e)$ and for all $k \in \mathbb{N} \cup \{0\}$.

We now summarise the properties of ψ_T, ψ_e and E in the following lemma (see [1, 49]).

LEMMA 4.3. *The following properties hold:*
(i) For $T \in \mathcal{T}_h$ and for $v \in \mathbb{P}_k(T)$, there is a positive constant C_1 such that

$$C_1^{-1} \|v\|_{0,T}^2 \leq \int_T \psi_T v^2 \, dx \leq C_1 \|v\|_{0,T}^2, \qquad C_1^{-1} \|v\|_{0,T}^2 \leq \|\psi v\|_{0,T}^2 + h_T^2 |\psi v|_{1,T}^2 \leq C_1 \|v\|_{0,T}^2.$$

(ii) For $e \in \mathcal{E}_h$ and $v \in \mathbb{P}_k(e)$, there exists a positive constant, say C_1, such that

$$C_1^{-1} \|v\|_{0,e}^2 \leq \int_e \psi_e v^2 \, ds \leq C_1 \|v\|_{0,e}^2.$$

(iii) For $T \in \mathcal{T}_h$, $e \in \mathcal{E}(T)$ and for $v \in \mathbb{P}_k(e)$, there is a positive constant, again say C_1, such that

$$\|\psi_e^{1/2} E(v)\|_{0,T}^2 \leq C_1 h_e \|v\|_{0,e}^2.$$

The following classical result which states an inverse estimate will also be used.

LEMMA 4.4. *Let $k, l, m \in \mathbb{N} \cup \{0\}$ such that $l \leq m$. Then, there exists $\tilde{C} > 0$, depending only on k, l, m and the shape regularity of the triangulations, such that for each triangle T there holds*

$$|q|_{m,T} \leq \tilde{C} h_T^{l-m} |q|_{l,T} \quad \forall q \in \mathbb{P}_k(T).$$

In order to prove the efficiency of the a posteriori error estimator, we will bound each term defining Θ_T in terms of local errors.

THEOREM 4.5. *There is a positive constant C_{eff}, independent of h, such that*

$$C_{\mathrm{eff}} \, \Theta \leq \ \|(\boldsymbol{u}, \omega) - (\boldsymbol{u}_h, \omega_h)\| + \|p - p_h\|_{0,\Omega} + \text{h.o.t.},$$

where h.o.t. denotes higher-order terms.

Proof. Using that $\omega - \mathbf{curl}\,\boldsymbol{u} = 0$ and $\operatorname{div}\boldsymbol{u} = 0$ in Ω (see (2.5b) and (2.5c), respectively), we immediately have that

$$\|\omega_h - \mathbf{curl}\,\boldsymbol{u}_h\|_{0,T} + \|\operatorname{div}\boldsymbol{u}_h\|_{0,T} \leq \|\mathbf{curl}(\boldsymbol{u} - \boldsymbol{u}_h)\|_{0,T} + \|\operatorname{div}(\boldsymbol{u} - \boldsymbol{u}_h)\|_{0,T} + \|\omega - \omega_h\|_{0,T}.$$

On the other hand, with the help of the $L^2(T)^2$-orthogonal projection $\mathcal{P}_T^\ell$ onto $\mathbb{P}_\ell(T)^2$, for $\ell \geq (s+k+1)$, with respect to the weighted L^2-inner product $(\psi_T \boldsymbol{f}, \boldsymbol{g})_{0,T}$, for $\boldsymbol{f}, \boldsymbol{g} \in L^2(T)^2$, it now follows that

$$\|\boldsymbol{f} - \sigma \boldsymbol{u}_h - \nu \,\mathbf{curl}\,\omega_h - (\boldsymbol{\beta}\cdot\nabla)\boldsymbol{u}_h + 2\varepsilon(\boldsymbol{u}_h)\nabla\nu - \nabla p_h\|_{0,T}^2$$
$$= \|\boldsymbol{f} - \mathcal{P}_T^\ell(\boldsymbol{f}) + \mathcal{P}_T^\ell(\boldsymbol{f}) - \sigma\boldsymbol{u}_h - \nu\,\mathbf{curl}\,\omega_h - (\boldsymbol{\beta}\cdot\nabla)\boldsymbol{u}_h + 2\varepsilon(\boldsymbol{u}_h)\nabla\nu - \nabla p_h\|_{0,T}^2$$
$$\leq \|\boldsymbol{f} - \mathcal{P}_T^\ell(\boldsymbol{f})\|_{0,T}^2 + \|\mathcal{P}_T^\ell(\boldsymbol{f}) - \sigma\boldsymbol{u}_h - \nu\,\mathbf{curl}\,\omega_h - (\boldsymbol{\beta}\cdot\nabla)\boldsymbol{u}_h + 2\varepsilon(\boldsymbol{u}_h)\nabla\nu - \nabla p_h\|_{0,T}^2$$
$$= \|\boldsymbol{f} - \mathcal{P}_T^\ell(\boldsymbol{f})\|_{0,T}^2 + \|\mathcal{P}_T^\ell(\boldsymbol{f} - \sigma\boldsymbol{u}_h - \nu\,\mathbf{curl}\,\omega_h - (\boldsymbol{\beta}\cdot\nabla)\boldsymbol{u}_h + 2\varepsilon(\boldsymbol{u}_h)\nabla\nu - \nabla p_h)\|_{0,T}^2.$$

For the second term on the right-hand side, an application of Lemma 4.3 shows that

$$\|\mathcal{P}_T^\ell(\boldsymbol{f} - \sigma\boldsymbol{u}_h - \nu\,\mathbf{curl}\,\omega_h - (\boldsymbol{\beta}\cdot\nabla)\boldsymbol{u}_h + 2\varepsilon(\boldsymbol{u}_h)\nabla\nu - \nabla p_h)\|_{0,T}^2$$
$$\leq \|\psi_T^{1/2}\mathcal{P}_T^\ell(\boldsymbol{f} - \sigma\boldsymbol{u}_h - \nu\,\mathbf{curl}\,\omega_h - (\boldsymbol{\beta}\cdot\nabla)\boldsymbol{u}_h + 2\varepsilon(\boldsymbol{u}_h)\nabla\nu - \nabla p_h)\|_{0,T}^2$$
$$= \int_T \psi_T \mathcal{P}_T^\ell(\boldsymbol{f} - \sigma\boldsymbol{u}_h - \nu\,\mathbf{curl}\,\omega_h - (\boldsymbol{\beta}\cdot\nabla)\boldsymbol{u}_h + 2\varepsilon(\boldsymbol{u}_h)\nabla\nu - \nabla p_h)$$

$$\times (\boldsymbol{f} - \sigma \boldsymbol{u}_h - \nu \operatorname{\mathbf{curl}} \omega_h - (\boldsymbol{\beta} \cdot \nabla)\boldsymbol{u}_h + 2\boldsymbol{\varepsilon}(\boldsymbol{u}_h)\nabla\nu - \nabla p_h),$$

where we have used the fact that $\mathcal{P}_T^\ell$ is the $L^2(T)^2$-orthogonal projection. Thus, from the above inequality, and (2.5a) (cf. Remark 2.5), we can deduce that

$$
\begin{aligned}
\|\mathcal{P}_T^\ell(\boldsymbol{f} &- \sigma \boldsymbol{u}_h - \nu \operatorname{\mathbf{curl}} \omega_h - (\boldsymbol{\beta} \cdot \nabla)\boldsymbol{u}_h + 2\boldsymbol{\varepsilon}(\boldsymbol{u}_h)\nabla\nu - \nabla p_h)\|_{0,T}^2 \\
&\leq \int_T \psi_T \mathcal{P}_T^\ell(\boldsymbol{f} - \sigma \boldsymbol{u}_h - \nu \operatorname{\mathbf{curl}} \omega_h - (\boldsymbol{\beta} \cdot \nabla)\boldsymbol{u}_h + 2\boldsymbol{\varepsilon}(\boldsymbol{u}_h)\nabla\nu - \nabla p_h) \\
&\quad \times (\sigma(\boldsymbol{u} - \boldsymbol{u}_h) + \nu \operatorname{\mathbf{curl}}(\omega - \omega_h) + (\boldsymbol{\beta} \cdot \nabla)(\boldsymbol{u} - \boldsymbol{u}_h) - 2\boldsymbol{\varepsilon}(\boldsymbol{u} - \boldsymbol{u}_h)\nabla\nu + \nabla(p - p_h)).
\end{aligned}
$$

Next, using that the viscosity is a polynomial function, the bound follows by integration by parts on the terms $\operatorname{\mathbf{curl}}(\omega - \omega_h)$ and $\nabla(p - p_h)$, Cauchy-Schwarz inequality and an inverse inequality (cf. Lemma 4.4). We end the proof by observing that the required efficiency bound follows straightforwardly from the estimates above, and after assuming additional regularity for $\boldsymbol{f}$. $\qquad\square$

5. Numerical results. In this section, we present some numerical experiments carried out with the schemes proposed and analysed in Section 3. We also present two numerical examples in $\mathbb{R}^2$, confirming the reliability and efficiency of the a posteriori error estimator Θ derived in Section 4, and showing the behaviour of the associated adaptive algorithm. The solution of all linear systems is carried out with the multifrontal massively parallel sparse direct solver MUMPS.

We construct a series of uniformly successively refined triangular meshes for Ω and compute individual errors

$$e(\boldsymbol{u}) = \|\boldsymbol{u} - \boldsymbol{u}_h\|_{1,\Omega}, \quad e(\boldsymbol{\omega}) = \|\boldsymbol{\omega} - \boldsymbol{\omega}_h\|_{0,\Omega}, \quad e(p) = \|p - p_h\|_{0,\Omega},$$

and convergence rates

$$r(\boldsymbol{u}) = \frac{\log(e(\boldsymbol{u})/\widehat{e}(\boldsymbol{u}))}{\log(h/\hat{h})}, \qquad r(\boldsymbol{\omega}) = \frac{\log(e(\boldsymbol{\omega})/\widehat{e}(\boldsymbol{\omega}))}{\log(h/\hat{h})}, \qquad r(p) = \frac{\log(e(p)/\widehat{e}(p))}{\log(h/\hat{h})}, \qquad (5.27)$$

where $e, \widehat{e}$ denote errors generated on two consecutive meshes of sizes $h, \hat{h}$, respectively.

5.1. Example 1: Convergence test using manufactured solutions. The first test consists of approximating closed-form solutions on a two-dimensional domain $\Omega = (0,1)^2$. We construct the forcing term $\boldsymbol{f}$ so that the exact solution to (2.5a)-(2.5c) is given by the following smooth functions

$$p(x,y) := \left(\left(x - \frac{1}{2}\right)^3 y^2 + (1-x)^3 \left(y - \frac{1}{2}\right)^3 \right),$$

$$\boldsymbol{u}(x,y) := \operatorname{\mathbf{curl}}(1000 x^2 (1-x)^4 y^3 (1-y)^2), \qquad \omega(x,y) := \operatorname{\mathbf{curl}} \boldsymbol{u},$$

which satisfy the incompressibility constraint as well as the boundary conditions. In addition, we take $\boldsymbol{\beta} = \boldsymbol{u}$, and two specifications for the variable viscosity are considered,

$$\nu_a(x,y) = \nu_0 + (\nu_1 - \nu_0)xy, \ \nu_b(x,y) = \nu_0 + (\nu_1 - \nu_0)exp(-10^{13}((x - 0.5)^{10} + (y - 0.5)^{10})),$$

with $\nu_0 = 0.001$, $\nu_1 = 1$, and taking $\kappa_1 = \frac{2}{3}\nu_0$, $\kappa_2 = \frac{\nu_0}{2}$ and $\sigma = 100$. The error history of the method introduced in Section 3.1.1 with discontinuous finite elements for vorticity $(\mathbf{W}_h^2)$ for $k = 1$ and for the two different viscosity functions is collected in Tables 5.1 and 5.2, respectively. These values indicate optimal accuracy $O(h^2)$ for $k = 1$, and for ν_a and ν_b, according to Theorem 3.2.

5.2. Example 2: Convergence in 3D. The aim of this numerical test is to assess the accuracy of the method in the 3D case. With this end, we consider the domain $\Omega := (0,1)^3$ and take $\boldsymbol{f}$ so that the exact solution is given by

$$p(x,y,z) := 1 - x^2 - y^2 - z^2, \quad \varphi(x,y,z) := x^2(1-x)^2 y^2(1-y)^2 z^2(1-z)^2,$$

$$\boldsymbol{u}(x,y,z) = \operatorname{\mathbf{curl}} \varphi, \qquad \boldsymbol{\omega}(x,y,z) = \operatorname{\mathbf{curl}} \boldsymbol{u},$$

h	$\lVert \boldsymbol{u} - \boldsymbol{u}_h \rVert_{1,\Omega}$	$r(\boldsymbol{u})$	$\lVert \omega - \omega_h \rVert_{0,\Omega}$	$r(\omega)$	$\lVert p - p_h \rVert_{0,\Omega}$	$r(p)$
0.7071	10.86	–	9.1110	–	2.5470	–
0.3536	4.4240	1.3	3.5500	1.4	1.5330	0.7
0.1768	1.2540	1.8	0.9854	1.9	0.3493	2.1
0.0883	0.3492	1.8	0.2470	2.0	0.0622	2.4
0.0441	0.1096	1.7	0.0613	2.0	0.0107	2.5
0.0221	0.0327	1.8	0.0151	2.0	0.0020	2.4
0.0110	0.0075	2.1	0.0037	2.0	0.0004	2.2

TABLE 5.1

Example 1: convergence tests against analytical solutions on a sequence of uniformly refined triangulations of the domain Ω and the viscosity function ν_a.

h	$\lVert \boldsymbol{u} - \boldsymbol{u}_h \rVert_{1,\Omega}$	$r(\boldsymbol{u})$	$\lVert \omega - \omega_h \rVert_{0,\Omega}$	$r(\omega)$	$\lVert p - p_h \rVert_{0,\Omega}$	$r(p)$
0.7071	10.91	–	9.1340	–	2.1190	–
0.3536	4.489	1.3	3.6710	1.3	1.4580	0.5
0.1768	1.367	1.7	1.1200	1.7	0.2789	2.4
0.0883	0.366	1.9	0.2951	1.9	0.0482	2.5
0.0441	0.113	1.7	0.0864	1.8	0.0070	2.8
0.0221	0.036	1.6	0.0220	2.0	0.0014	2.3
0.0110	0.007	2.1	0.0046	2.2	0.0003	2.2

TABLE 5.2

Example 1: convergence tests against analytical solutions on a sequence of uniformly refined triangulations of the domain Ω and the viscosity function ν_b.
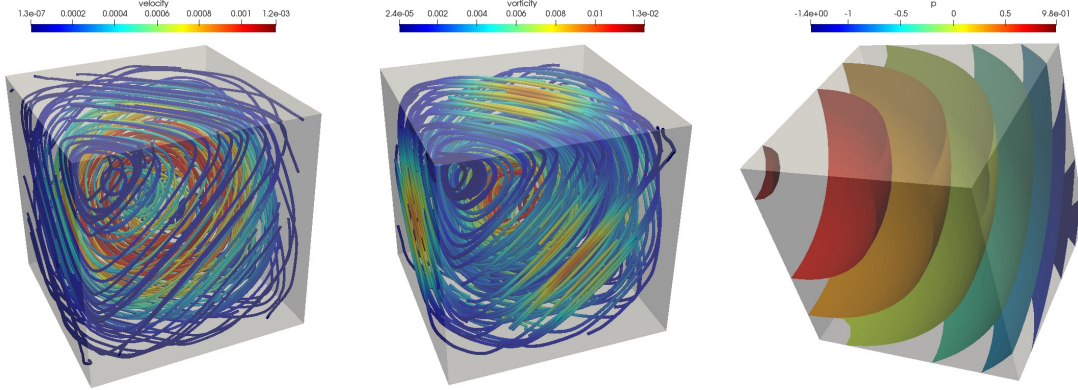

FIG. 5.1. *Example 2: Approximate solutions computed using the MINI-element. Velocity streamlines (left) vorticity streamlines (centre) and pressure distribution (right).*

and we consider $\boldsymbol{\beta} = \boldsymbol{u}$, and $\nu_c(x,y,z) = \nu_0 + (\nu_1 - \nu_0)x^2 y^2 z^2$. The remaining constants are $\nu_0 = 0.1$, $\nu_1 = 1$, $\kappa_1 = \frac{2}{3}\nu_0$, $\kappa_2 = \frac{\nu_0}{2}$, and $\sigma = 1000$. We observe that the hypothesis of Lemma 2.2 are satisfied. Additionally, we employ finite elements with $k = 1$, that is, $\mathbf{V}_h$ approximating the velocity, and piecewise linear and continuous elements for vorticity and pressure.

In Table 5.3, we summarise the convergence history for a sequence of uniform meshes. For velocity we observe the $O(h)$ convergence predicted by Theorem 3.3, whereas the approximation of vorticity and pressure seem to be superconvergent. Figure 5.1 displays velocity and vorticity streamlines as well as the approximate pressure distribution.

5.3. Example 3: A posteriori error estimates and adaptive mesh refinement. In this numerical test, we test the efficiency of the a posteriori error estimator (4.22) and applying mesh refinement according to the local value of the indicator. In this case, the convergence rates are obtained by replacing the expression $\log(h/\hat{h})$ appearing in the computation of (5.27) by $-\frac{1}{2}\log(N/\hat{N})$,

t

h	$\|\boldsymbol{u} - \boldsymbol{u}_h\|_{1,\Omega}$	$r(\boldsymbol{u})$	$\|\boldsymbol{\omega} - \boldsymbol{\omega}_h\|_{0,\Omega}$	$r(\boldsymbol{\omega})$	$\|p - p_h\|_{0,\Omega}$	$r(p)$
0.866	0.01021	–	0.00299	–	0.04732	–
0.433	0.00858	0.3	0.00125	1.3	0.01399	1.8
0.288	0.00665	0.6	0.00067	1.5	0.00572	2.2
0.216	0.00513	0.9	0.00043	1.5	0.00290	2.4
0.173	0.00398	1.1	0.00030	1.5	0.00171	2.4
0.144	0.00313	1.3	0.00023	1.5	0.00112	2.3
0.123	0.00251	1.3	0.00018	1.5	0.00079	2.2

TABLE 5.3

Example 2: experimental convergence using homogeneous Dirichlet boundary conditions on a 3D domain Ω and using the viscosity function ν_c.
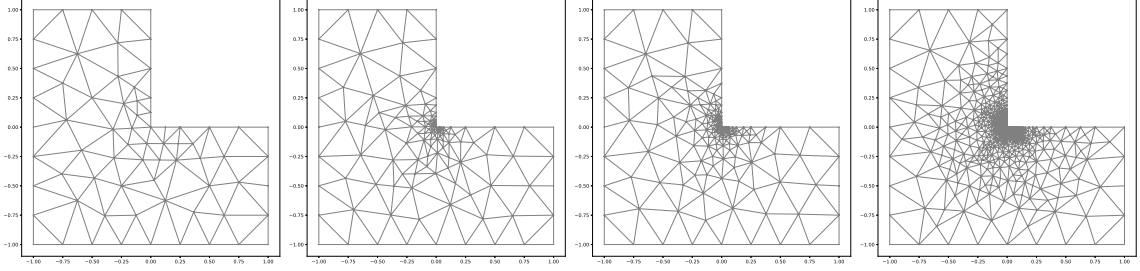

FIG. 5.2. *Example 3: Snapshots of four grids, $\mathcal{T}_h^1$, $\mathcal{T}_h^4$, $\mathcal{T}_h^6$, $\mathcal{T}_h^{10}$, adaptively refined according to the a posteriori error indicator defined in* (4.22).

where N and $\hat{N}$ denote the corresponding degrees of freedom of each triangulation.

Now, we recall the definition of the so-called effectivity index as the ratio between the total error and the global error estimator, i.e.,

$$\mathtt{e}(\boldsymbol{u}, \omega, p) := \left\{ [e(\boldsymbol{u})]^2 + [e(\omega)]^2 + [e(p)]^2 \right\}^{1/2}, \qquad \mathtt{eff}(\Theta) := \frac{\mathtt{e}(\boldsymbol{u}, \omega, p)}{\Theta}.$$

We will employ the family of finite elements introduced in Section 3.1.1 for $k = 1$, namely piecewise quadratic and continuous elements for velocity and piecewise linear and continuous elements for vorticity and pressure fields.

The computational domain is the nonconvex L-shaped domain $\Omega = (-1, 1)^2 \setminus (0, 1)^2$, where problem (2.5a)-(2.5c) admits the following exact solution

$$p(x, y) := \frac{1 - x^2 - y^2}{(x - 0.025)^2 + (y - 0.025)^2} - 12.742942014/3,$$

$$\varphi(x, y) = x^2(1 - x)^2 y^2 (1 - y)^2 \exp(-50((x - 0.025)^2 + (y - 0.025)^2)), \quad \boldsymbol{u} = \mathbf{curl}\,\varphi, \quad \omega = \mathbf{curl}\,\boldsymbol{u},$$

which satisfy the incompressibility constraint as well as the boundary conditions. Convective velocity, viscosity, and other parameters are taken as

$$\boldsymbol{\beta} = \boldsymbol{u}, \quad \nu_d(x, y) = \nu_0 + \frac{721}{16}(\nu_1 - \nu_0)x^2(1 - x)y^2(1 - y), \quad \nu_0 = 0.1, \quad \nu_1 = 1,$$

$$\nu_e(x, y) = \nu_0 + (\nu_1 - \nu_0)\exp(-10^{12}((x - 0.5)^{10} + (y - 0.5)^{10})), \quad \kappa_1 = \frac{2}{3}\nu_0, \quad \kappa_2 = \frac{\nu_0}{2}, \quad \sigma = 10.$$

Pressure is singular near the reentrant corner of the domain and so we expect hindered convergence of the approximations when a uniform (or quasi-uniform) mesh refinement is applied. In contrast, if we apply the following adaptive mesh refinement procedure from [49]:

1) Start with a coarse mesh $\mathcal{T}_h$.
2) Solve the discrete problem (3.17) for the current mesh $\mathcal{T}_h$.
3) Compute $\Theta_T := \Theta$ for each triangle $T \in \mathcal{T}_h$.

N	$\|\boldsymbol{u} - \boldsymbol{u}_h\|_{1,\Omega}$	$r(\boldsymbol{u})$	$\|\omega - \omega_h\|_{0,\Omega}$	$r(\omega)$	$\|p - p_h\|_{0,\Omega}$	$r(p)$	$\texttt{eff}(\Theta)$
661	49.68	–	8.821	–	6.685	–	1.133
999	32.37	2.07	5.069	2.68	3.985	2.50	1.157
1241	15.46	6.81	2.104	8.10	1.846	7.09	1.144
1881	9.058	2.57	1.396	1.97	1.057	2.68	1.098
2103	7.178	4.17	0.907	7.72	0.828	4.36	1.135
2621	5.645	2.18	0.754	1.67	0.655	2.12	1.120
3851	3.647	2.27	0.454	2.63	0.418	2.33	1.168
4267	3.243	2.29	0.401	2.46	0.365	2.61	1.156
5271	2.687	1.77	0.298	2.76	0.294	2.03	1.143
7819	1.754	2.16	0.194	2.18	0.191	2.22	1.155

TABLE 5.4

Example 3: Convergence history and effectivity indexes for the method introduced in Section 3.1.1, computed on a sequence of adaptively refined triangulations of the L-shaped domain and using viscosity ν_d.

N	$\|\boldsymbol{u} - \boldsymbol{u}_h\|_{1,\Omega}$	$r(\boldsymbol{u})$	$\|\omega - \omega_h\|_{0,\Omega}$	$r(\omega)$	$\|p - p_h\|_{0,\Omega}$	$r(p)$	$\texttt{eff}(\Theta)$
661	49.73	–	8.842	–	6.681	–	1.132
999	32.39	2.07	5.081	2.68	3.980	2.50	1.155
1241	15.50	6.79	2.122	8.05	1.838	7.12	1.138
1881	9.087	2.56	1.401	1.99	1.039	2.74	1.085
2103	7.213	4.14	0.914	7.65	0.806	4.55	1.114
2589	5.683	2.29	0.759	1.78	0.633	2.32	1.112
3771	3.734	2.23	0.461	2.64	0.406	2.35	1.113
5161	2.674	2.12	0.307	2.58	0.287	2.20	1.108
6867	1.946	2.22	0.207	2.77	0.205	2.36	1.116
9887	1.346	2.02	0.128	2.60	0.138	2.16	1.119

TABLE 5.5

Example 3: Convergence history and effectivity indexes for the method introduced in Section 3.1.1, computed on a sequence of adaptively refined triangulations of the L-shaped domain and using viscosity ν_e.

4) Check the stopping criterion and decide whether to finish or go to next step.

5) Use *blue-green* refinement on those $T' \in \mathcal{T}_h$ whose indicator $\Theta_{T'}$ satisfies

$$\Theta_{T'} \geq \frac{1}{2} \max_{T \in \mathcal{T}_h} \left\{ \Theta_T : T \in \mathcal{T}_h \right\} .$$

6) Define resulting meshes as current meshes $\mathcal{T}_h$ and $\mathcal{T}_h$, and go to step 2,

we expect a recovering of the optimal convergence rates. In fact, this can be observed from the bottom rows of Tables 5.4 and 5.5, for both ν_d and ν_e, respectively. Moreover, the efficiency indexes are around 1 for both viscosities. The resulting meshes after a few adaptation steps are reported in Figure 5.2, showing the expected refinement near the reentrant corner.

5.4. Example 4: Steady blood flow in aortic arch. We finalise the set of examples with a simple simulation of pseudo-stationary blood flow in an aorta. The patient-specific geometry [38, 39] has one inlet (a segment that connects with the pre-aortic root coming from the aortic valve in the heart) and four outlets (the left common carotid artery, the left subclavian artery, the innominate artery, and the larger descending aorta). On the inlet we impose a Poiseuille profile of magnitude 4, on the vessel walls we set no-slip conditions, and on the remaining boundaries we set zero normal stresses (more physiologically relevant boundary conditions can be considered following, e.g., [24, 32]). The initial unstructured mesh has 46352 tetrahedral elements. The synthetic variable viscosity field is a smooth exponential function $\nu = \nu_0 + (\nu_1 - \nu_0) \exp(-10^3[(x - 0.1)^6 + y - 0.5)^6 + (z - 0.5)^6])$ with $\nu_0 = 10^{-3}, \nu_1 = 10$ that entails an average Reynolds number of approximately 60 (computed using the inlet diameter and maximal inlet velocity), while the convecting velocity is computed as the solution of a preliminary Stokes problem (on the initial coarse mesh), and we prescribe $\sigma = 1000$ and $\boldsymbol{f} = \sigma\boldsymbol{\beta}$. Then we compute numerical solutions of the Oseen problem
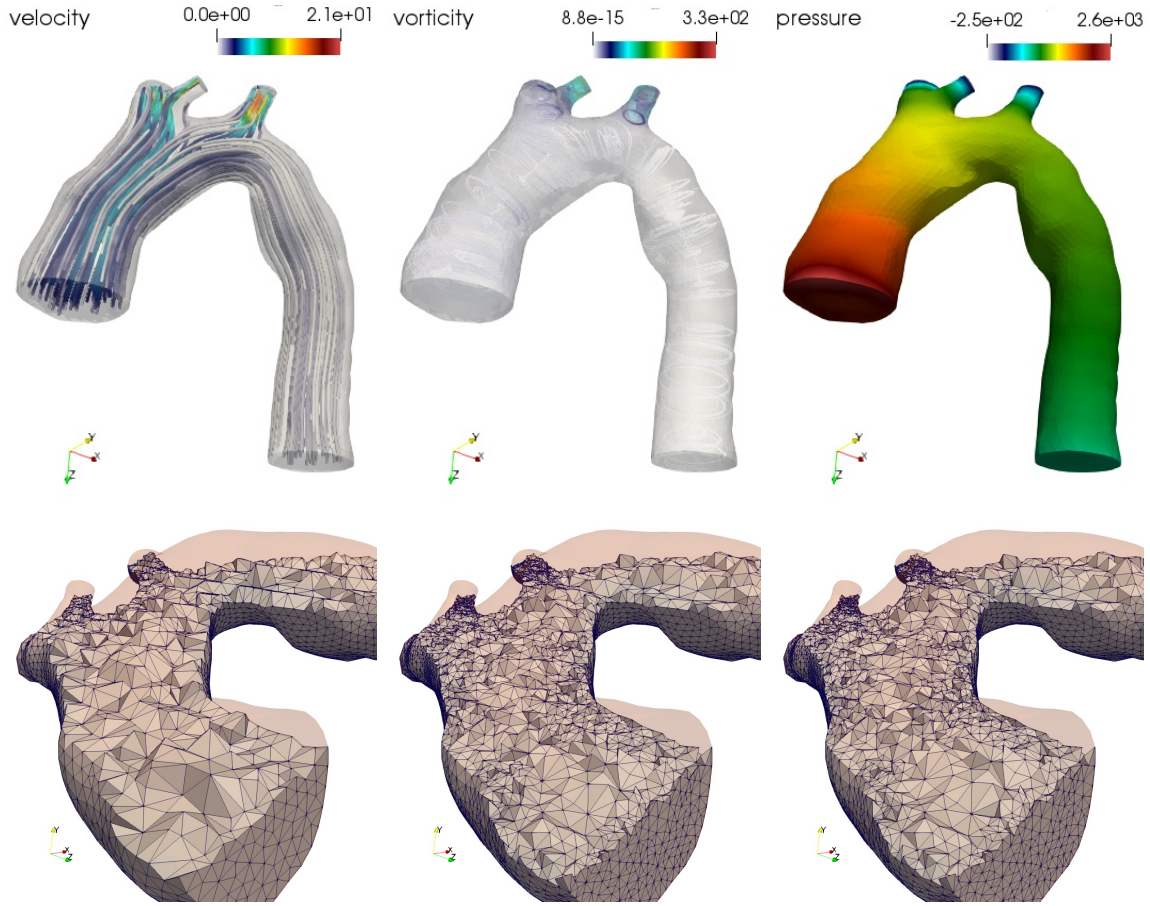
FIG. 5.3. *Example 4: Simulation of stationary blood flow in an aortic arch. Approximate velocity, vorticity, and pressure (top panels), and samples of adaptive mesh after one, two and three refinement steps, and visualising a cut focusing on the boundaries (bottom row).*

and apply four steps of adaptive mesh refinement using a 3D version of the estimator (4.22) and the algorithm described in the previous example. The results are portrayed in Figure 5.3, plotting pressure distribution, velocity streamlines, vorticity, and a sample of the resulting adaptive mesh which shows more refinement near the boundaries of the descending aorta. For this test we have used a conforming approximation of vorticity.

REFERENCES

[1] M. AINSWORTH AND J.T. ODEN, *A posteriori error estimation in finite element analysis.* Wiley, New York, 2000.

[2] M. ALVAREZ, G.N. GATICA, AND R. RUIZ-BAIER, *A vorticity-based fully-mixed formulation for the 3D Brinkman-Darcy problem*, Comput. Methods Appl. Mech. Engrg., 307 (2016) 68–95.

[3] M. AMARA, D. CAPATINA-PAPAGHIUC, AND D. TRUJILLO, *Stabilized finite element method for Navier-Stokes equations with physical boundary conditions*, Math. Comp., 76(259) (2007) 1195–1217.

[4] M. AMARA, E. CHACÓN VERA, AND D. TRUJILLO, *Vorticity–velocity–pressure formulation for Stokes problem*, Math. Comp., 73(248) (2004) 1673–1697.

[5] V. ANAYA, A. BOUHARGUANE, D. MORA, C. REALES, R. RUIZ-BAIER, N. SELOULA AND H. TORRES, *Analysis and approximation of a vorticity-velocity-pressure formulation for the Oseen equations*, J. Sci. Comput., 88(3) (2019) 1577–1606.

[6] V. ANAYA, B. GÓMEZ-VARGAS, D. MORA AND R. RUIZ-BAIER, *Incorporating variable viscosity in vorticity-based formulations for Brinkman equations*, C. R. Math. Acad. Sci. Paris, 357(6) (2019) 552–560.

[7] V. ANAYA, D. MORA, R. OYARZÚA, AND R. RUIZ-BAIER, *A priori and a posteriori error analysis of a mixed scheme for the Brinkman problem*, Numer. Math., 133(4) (2016) 781-817.

[8] V. ANAYA, D. MORA, AND R. RUIZ-BAIER, *An augmented mixed finite element method for the vorticity-velocity-pressure formulation of the Stokes equations*, Comput. Methods Appl. Mech. Engrg., 267 (2013) 261–274.

[9] T.P. BARRIOS, J.M. CASCÓN AND M. GONZÁLEZ, *Augmented mixed finite element method for the Oseen problem:*

a priori and a posteriori error analyses, Comput. Methods Appl. Mech. Engrg., 313 (2017) 216–238.

[10] M. Benzi, and M.A. Olshanskii, *An augmented Lagrangian-based approach to the Oseen problem,* SIAM J. Sci. Comput., 28(6) (2006) 2095–2113.

[11] M. Benzi, M.A. Olshanskii, L.G. Rebholz and Z. Wang, *Assessment of a vorticity based solver for the Navier–Stokes equations,* Comput. Methods Appl. Mech. Engrg., 247-248 (2012) 216–225.

[12] C. Bernardi, and N. Chorfi, *Spectral discretization of the vorticity, velocity, and pressure formulation of the Stokes problem*, SIAM J. Numer. Anal., 44(2) (2006) 826–850.

[13] P.V. Bochev, *Analysis of least-squares finite element methods for the Navier–Stokes equations*, SIAM J. Numer. Anal., 34(5) (1997) 1817–1844.

[14] P.V. Bochev, and M. Gunzburger, *Least-Squares finite element methods*. Volume 166 of Applied Mathematical Sciences. Springer Verlag (2009).

[15] D. Boffi, *Stability of higher order triangular Hood–Taylor methods for stationary Stokes equations*, Math. Models Methods Appl. Sci., 2(4) (1994) 223–235.

[16] D. Boffi, F. Brezzi, and M. Fortin, *Mixed Finite Element Methods and applications*. Springer Series in Computational Mathematics, 44. Springer, Heidelberg (2013).

[17] Z. Cai and B. Chen, *Least-squares method for the Oseen equation*, Numer. Methods Partial Differential Equations, 32 (2016) 1289–1303.

[18] J. Camaño, R. Oyarzúa, R. Ruiz-Baier, and G. Tierra, *Error analysis of an augmented mixed method for the Navier-Stokes problem with mixed boundary conditions*, IMA J. Numer. Anal., 38(3) (2018) 1452–1484.

[19] J.O. Campos, R. Weber dos Santos, J. Sundnes, and B. Martins Rocha, *Preconditioned augmented Lagrangian formulation for nearly incompressible cardiac mechanics*, Int. J. Numer. Methods Biomed. Engrg., 34(4) (2018) e2948.

[20] C.L. Chang, and B.-N. Jiang, *An error analysis of least-squares finite element method of velocity-pressure-vorticity formulation for the Stokes problem*, Comput. Methods Appl. Mech. Engrg., 84(3) (1990) 247–255.

[21] C.L. Chang and S.-Y. Yang, *Analysis of the $[L^2, L^2, L^2]$ least-squares finite element method for incompressible Oseen-type problems,* Int. J. Numer. Anal. Model., 4(3-4) (2007) 402–424.

[22] P. Clément, *Approximation by finite element functions using local regularisation*, RAIRO Modél. Math. Anal. Numer., 9 (1975) 77–84.

[23] B. Cockburn, and J. Cui, *An analysis of HDG methods for the vorticity-velocity-pressure formulation of the Stokes problem in three dimensions*, Math. Comp., 81(279) (2012) 1355–1368.

[24] T. Dobroserdova, F. Liang, G. Panasenko, and Y. Vassilevski, *Multiscale models of blood flow in the compliant aortic bifurcation*, Appl. Math. Letters, 93C (2019) 98–104.

[25] H.-Y. Duan, and G.-P. Liang, *On the velocity-pressure-vorticity least-squares mixed finite element method for the 3D Stokes equations*, SIAM J. Numer. Anal., 41(6) (2003) 2114–2130.

[26] F. Dubois, M. Salaün, and S. Salmon, *First vorticity-velocity-pressure numerical scheme for the Stokes problem*, Comput. Methods Appl. Mech. Engrg., 192(44–46) (2003) 4877–4907.

[27] A. Ern, *Vorticity-velocity formulation of the Stokes problem with variable density and viscosity*, Math. Models Methods Appl. Sci., 8(2) (1998) 203–218.

[28] A. Ern and J.-L. Guermond, Theory and Practice of Finite Elements. Applied Mathematical Sciences. Springer-Verlag, (2004).

[29] P.E. Farrell, L.F. Gatica, B.P. Lamichhane, R. Oyarzúa, and R. Ruiz-Baier, *Mixed Kirchhoff stress - displacement - pressure formulations for incompressible hyperelasticity*, Comput. Methods Appl. Mech. Engrg., 374 (2021) e113562.

[30] P.E. Farrell, and P.A. Gazca-Orozco, *An augmented Lagrangian preconditioner for implicitly constituted non-Newtonian incompressible flow,* SIAM J. Sci. Comput., 42(6) (2020) B1329–B1349.

[31] P.E. Farrell, L. Mitchell, and F. Wechsung, *An augmented Lagrangian preconditioner for the 3D stationary incompressible Navier-Stokes equations at high Reynolds number,* SIAM J. Sci. Comput., 41(5) (2019) A3073–A3096.

[32] L Formaggia, J.F. Gerbeau, F. Nobile, and A. Quarteroni, *Numerical treatment of defective boundary conditions for the Navier-Stokes equations*, SIAM J. Numer. Anal., 40 (2002) 376–401.

[33] G.N. Gatica, *A Simple Introduction to the Mixed Finite Element Method. Theory and Applications*. Springer Briefs in Mathematics, Springer, Cham Heidelberg New York Dordrecht London (2014).

[34] G.N. Gatica, R. Oyarzúa, and N. Valenzuela, *A five-field augmented fully-mixed finite element method for the Navier-Stokes/Darcy coupled problem*, Comput. Math. Appl., 80(8) (2020) 1944–1963.

[35] V. Girault, and P.A. Raviart, *Finite element methods for Navier-Stokes equations. Theory and Algorithms*. Springer-Verlag, Berlin (1986).

[36] P. Hood, and C. Taylor, *Numerical solution of the NavierStokes equations using the finite element technique*, Comput. Fluids, 1 (1973) 1–28

[37] V. John, K. Kaiser, and J. Novo, *Finite element methods for the incompressible Stokes equations with variable viscosity*, ZAMM Z. Angew. Math. Mech., 96(2) (2016) 205–216.

[38] E. Marchandise, P. Crosetto, C. Geuzaine, J.-F. Remacle, and E. Sauvage, *Quality open source mesh generation for cardiovascular flow simulation*. In: D. Ambrosi, A. Quarteroni, and G. Rozza, editors. Modeling of Physiological Flows. Milano: Springer (2011) 395–414.

[39] E. Marchandise, E. Sauvage, and J.-F. Remacle, *Quality open source mesh generation for biological flow simulations*. In: Proceedings of the ECCOMAS Thematic International Conference on Simulation and Modeling of Biological Flows (SIMBIO 2011) September 21-23, 2011, VUB, Brussels, Belgium.

[40] S. Mohapatra, and S. Ganesan, *A non-conforming least squares spectral element formulation for Oseen equations with applications to Navier-Stokes equations,* Numer. Funct. Anal. Optim., 37(10) (2016) 295–1311.

[41] P.R. Patil, and G. Vaidyanathan, *Effect of variable viscosity on thermohaline convection in a porous medium*, J. Hydrology, 57(1-2) (1982) 147–161.

[42] L.E. Payne, J.C. Song, and B. Straughan, *Continuous dependence and convergence results for Brinkman and Forchheimer models with variable viscosity*, Proc. Royal Soc. London Series A, 455 (1986) 1–20.

[43] J.P. Pontaza, and J.N. Reddy, *Spectral/hp least-squares finite element formulation for the Navier-Stokes equations*, J. Comput. Phys., 190(2) (2003) 523–549.

[44] J. Rudi, G. Stadler, and O. Ghattas, *Weighted BFBT preconditioner for Stokes flow problems with highly heterogeneous viscosity*, SIAM J. Sci. Comput., 39(5) (2017) S272–S297.

[45] M. Salaün, and S. Salmon, *Numerical stabilization of the Stokes problem in vorticity-velocity-pressure formulation*, Comput. Methods Appl. Mech. Engrg., 196(9-12) (2007) 1767–1786.

[46] M. Salaün, and S. Salmon, *Low-order finite element method for the well-posed bidimensional Stokes problem*, IMA J. Numer. Anal., 35 (2015) 427–453.

[47] C.G. Speziale, *On the advantages of the vorticity-velocity formulations of the equations of fluid dynamics*, J. Comput. Phys., 73(2) (1987) 476–480.

[48] C.-C. Tsai, and S.-Y. Yang, *On the velocity-vorticity-pressure least-squares finite element method for the stationary incompressible Oseen problem,* J. Comput. Appl. Math., 182(1) (2005) 211–232.

[49] R. Verfürth, *A review of a posteriori error estimation and adaptive-mesh-refinement techniques.* Wiley-Teubner, Chichester (1996).